Check for updates

New Phytologist

Research

Atmospheric dust is a global nutrient source for plants via foliar uptake

Anton Lokshin[1], Daniel Palchan[2], Marcelo Sternberg[3], Tom Goren[4], Mahdi (André) Nakhavali[5] and Avner Gross[1]

[1]The Department of Environmental, Geoinformatics and Urban Planning Sciences, Ben Gurion University of the Negev, Be'er Sheva, 8410501, Israel; [2]The Department of Civil Engineering, Ariel University, Ariel, 40700, Israel; [3]School of Plant Sciences and Food Security, Faculty of Life Sciences, Tel Aviv University, Tel Aviv, 6997820, Israel; [4]Department of Environment, Planning and Sustainability, Bar-Ilan University, Ramat Gan, 5290002, Israel; [5]International Institute for Applied Systems Analysis (IIASA), Laxenburg, A-2361, Austria

Author for correspondence:
Anton Lokshin
Email: lokshinanton@gmail.com

Received: *16 November 2025*
Accepted: *21 February 2026*

New Phytologist (2026)
doi: 10.1111/nph.71112

Key words: atmospheric deposition, desert dust, foliar uptake, natural Mediterranean ecosystem, phosphorus, plant nutrition.

Summary

- Atmospheric mineral dust is a critical nutrient supplier to marine ecosystems, but its role in terrestrial plant nutrition remains underexplored due to the assumption that nutrients are acquired solely from soils via roots.
- Here, we demonstrate that plants directly acquire nutrients from dust through leaves, revealing an unrecognized terrestrial uptake pathway. In a Mediterranean field study simulating dust events, dust application markedly increased plant macro and micronutrient concentrations, facilitated by the mildly acidic, organic-acid-rich leaf microenvironment that enhances dust dissolution and nutrient release.
- By integrating field observations with dust deposition estimates and soil nutrient data from different regions, we find that annual dust-derived inputs through leaves can account for up to 17% of soil-derived iron fluxes in the Western United States and up to 12% of phosphorus fluxes in the Eastern Amazon. During Mediterranean dust events, daily nutrient inputs can match or exceed soil-derived fluxes.
- Our findings suggest the major plant nutrition role of foliar dust uptake in nutrient-poor and dust-affected ecosystems. Such a foliar absorption pathway may become increasingly important as dust emissions and transport shift under future climate change and should be accounted for in vegetation, nutrients, and carbon-cycle models.

Introduction

Every year, billions of tons of mineral dust particles are lifted by winds from arid, unvegetated areas and transported across the globe (Kok *et al.*, 2021, 2023), where they impact atmospheric processes and global climate (Kok *et al.*, 2017; Adebiyi & Kok, 2020; Barr *et al.*, 2023; Villanueva *et al.*, 2025) and redistribute life-sustaining elements thousands of kilometers from their source (Chadwick *et al.*, 1999; Pett-Ridge, 2009; Brahney *et al.*, 2024; Molina Catricheo *et al.*, 2024). After deposition, dust particles can fertilize marine and terrestrial ecosystems by supplying macronutrients such as phosphorus (P), potassium (K), and magnesium (Mg), along with micronutrients like iron (Fe), manganese (Mn), copper (Cu) and nickel (Ni) (Chadwick *et al.*, 1999; Pett-Ridge, 2009; Gross *et al.*, 2016; Mahowald *et al.*, 2018; Lu *et al.*, 2024). Most research on dust fertilization has focused on marine ecosystems, where episodic dust events deliver pulses of P and micronutrients that are otherwise scarce in seawater, triggering immediate impacts on biological productivity (Jickells *et al.*, 2005; Westberry *et al.*, 2023; Matzenbacher *et al.*, 2024; Weis *et al.*, 2024). Experimental dust additions have shown rapid nutritional responses in marine life, altering nutrient status, growth rates, and physiology of phytoplankton and coral communities (Rubin *et al.*, 2011; Guieu *et al.*, 2014; Blanckaert *et al.*, 2022). On land, soil is classically viewed as the sole nutrient source to plants, and dust deposition impacts are considered relevant only over the millennial time scale, influencing long-term soil development and physicochemical properties while slowly replenishing soil nutrient stocks (Chadwick *et al.*, 1999; Pett-Ridge, 2009; Arvin *et al.*, 2017; Palchan *et al.*, 2018; Brahney *et al.*, 2024). The direct nutritional role of dust pulses to terrestrial vegetation is challenging to detect, especially against the large background of soil nutrients and the difficulty of distinguishing fresh dust inputs from existing soil pools. However, a substantial fraction of deposited dust does not immediately reach the soil, but is intercepted by plant foliage due to its large surface area and complex leaf architecture, which amplifies the interception of atmospheric particles over the ecosystem by several orders of magnitude (Blanusa *et al.*, 2015; Uni & Katra, 2017; Bauters *et al.*, 2021). Although some dust may ultimately be washed from the leaf surface to the soil, its prolonged and direct contact with foliage concentrates deposition onto plant tissues, bypassing soil-mediated immobilization and reducing interspecific competition. Additionally, leaf surfaces create a distinct chemical

© 2026 The Author(s).
New Phytologist © 2026 New Phytologist Foundation.
This is an open access article under the terms of the Creative Commons Attribution-NonCommercial-NoDerivs License, which permits use and distribution in any medium, provided the original work is properly cited, the use is non-commercial and no modifications or adaptations are made.

environment (slightly acidic, with organic acids) that enhances the dissolution of nutrients that are otherwise poorly soluble in soils (Fernandez & Eichert, 2009; Gross *et al.*, 2021; Golan *et al.*, 2025). Consequently, the actual availability of dust-borne nutrients to plants may be greater than previously assumed, particularly if considering direct foliar uptake. While foliar uptake is widely recognized as an effective nutrient feeding strategy in crops (Bukovac & Wittwer, 1957), the link between the foliar pathway and ecology is overlooked, and no field study has demonstrated its significance in natural ecosystems or quantified its contribution globally. Our work fills this gap, overturning the soil-centric paradigm of terrestrial plant nutrition. In previous studies, we identified and quantified foliar uptake of dust-borne nutrients by various tree species and crop plants in controlled conditions (Gross *et al.*, 2021; Starr *et al.*, 2023; Lokshin *et al.*, 2024a, 2025).

To investigate the contribution of mineral dust to plants' nutrition and the role of the foliar uptake, we conducted an *in situ* dust application experiment in a natural Mediterranean shrubland (Alon & Sternberg, 2019). The site receives high annual mineral dust deposition from the Arabian and Sahara deserts (*c.* 100 g m^{-2} yr^{-1}) (Ganor *et al.*, 2010; Kok *et al.*, 2021) and lies on alkaline and well-aerated soil that restricts nutrient bioavailability due to low solubility under high pH and redox conditions (Supporting Information Tables S1, S2). On an annual basis, dust-derived nutrient inputs are often obscured by dominant soil nutrient fluxes, but because dust deposition is episodic and confined to a limited number of intense events per year (typically 15–30 d; Ganor *et al.*, 2010), the flux of bioavailable nutrients during dust days can potentially match other sources (Gross *et al.*, 2016). We experimentally simulated dust events during the regional dust season by applying three discrete dust pulses onto the foliage of *Cistus creticus*, *Salvia fruticosa*, and *Teucrium capitatum*, three widespread plant species at the study site (Alon & Sternberg, 2019). Dust was applied as dry deposition, the dominant mode in the Eastern Mediterranean. To trace the nutritional contribution of dust to plants and distinguish between dust-derived and soil-derived nutrient uptake, we used volcanic mineral dust with a unique Rare Earth Element signature (REEs), distinct from local soils (Lokshin *et al.*, 2025).

Materials and Methods

Study site

The experiment was conducted at the Matta Long-Term Ecological Research (LTER) station in the Judean Hills, Israel (Fig. 1; 31°42′N, 35°03′E; 620 m asl; Alon & Sternberg, 2019). The site experiences a Mediterranean climate with warm, dry summers and mild, wet winters, receiving an average annual precipitation of 540 mm (Adar & Sternberg, 2026). The mean annual temperature is 17.7°C. The soil is classified as terra rossa, formed on hard limestone and chalk, with 5.2% organic carbon, 0.43% total nitrogen, and 6.8 mg kg^{-1} available P (Olsen P), and an average pH of 7.85 (Table S1). The site receives *c.* 100 g m^{-2} yr^{-1} of atmospheric dust deposition, mostly as dry deposition, primarily sourced from the Sahara and Arabian deserts via synoptic-scale transport events (Ganor & Foner, 2001; Ganor *et al.*, 2010; Kok *et al.*, 2021). To assess the relatively mobile nutrient reservoirs in the soils, surface soils were digested with 1 M HNO_3. These analyses revealed relatively high concentrations of P and of micronutrients such as Fe, Mn, Ni, and Cu. However, diethylenetriaminepentaacetic acid (DTPA) and Olsen extractions, which are considered a representation of the readily bioavailable fractions of micronutrients and P, respectively (Lindsay & Norvell, 1978), indicate that their availability to plants is limited (Tables S1, S2). This is consistent with global-scale patterns of low micronutrient availability in Mediterranean alkaline soils (Moreno-Jiménez *et al.*, 2019; Ochoa-Hueso *et al.*, 2023). For the chemical and elemental data of soils and dust used in this study, see Tables S4 and S5.

Plant species selection

The local vegetation in the study site is a species-rich Mediterranean dwarf-shrubland dominated by *Sarcopoterium spinosum* (L.) Spach and *Cistus creticus* L., interspersed with seasonal herbaceous species that flourish during the rainy season. Over 250 plant species were identified within the experimental plots, with herbaceous annuals covering up to 90% of open areas at peak biomass (March to April) and contributing to *c.* 50% of the annual net primary productivity (Tielbörger *et al.*, 2014; Alon & Sternberg, 2019). Mediterranean shrub species are generally reported to be hypostomatous, with stomata predominantly located on the abaxial leaf surface, a common trait associated with adaptation to seasonal drought (Galmés *et al.*, 2006). Within this community, three widespread Mediterranean perennial shrubs, *Cistus creticus* L., *Salvia fruticosa* Mill., and *Teucrium capitatum* L., were selected for the study. These species are well represented at the site and are known for their distinctive leaf surface traits, such as dense pubescence, which enhances dust particle adherence and may promote nutrient solubilization through the secretion of organic acids (Mo *et al.*, 2015; Gross *et al.*, 2021; Lokshin *et al.*, 2025).

Dust type

Dust of volcanic origin was used in this study as a natural dust analog to enable controlled and reproducible application under field conditions. Also, the volcanic dust REE pattern is compositionally distinct from dust sources with sedimentary or granitic origin, and from the pattern of soils in the study site, which exhibit a characteristic signature shaped by the long-term accumulation of Saharan dust at the site (Moreno *et al.*, 2006; Palchan *et al.*, 2018). Although volcanic dust can differ in mineralogy and elemental ratios from sedimentary-derived dust, our previous work demonstrated that both volcanic and non-volcanic dust produce comparable effects on plant nutrient uptake and biomass accumulation when applied to leaves under controlled conditions (Lokshin *et al.*, 2024a, 2025). Moreover, the macro- and micronutrient concentrations of the dust analog fall within the range reported for Saharan and Arabian desert dusts (Gross *et al.*, 2015;

© 2026 The Author(s).
New Phytologist © 2026 New Phytologist Foundation.

14698137, 0, Downloaded from https://nph.onlinelibrary.wiley.com/doi/10.1111/nph.71112 by CochraneAustria, Wiley Online Library on [08/04/2026]. See the Terms and Conditions (https://onlinelibrary.wiley.com/terms-and-conditions) on Wiley Online Library for rules of use; OA articles are governed by the applicable Creative Commons License

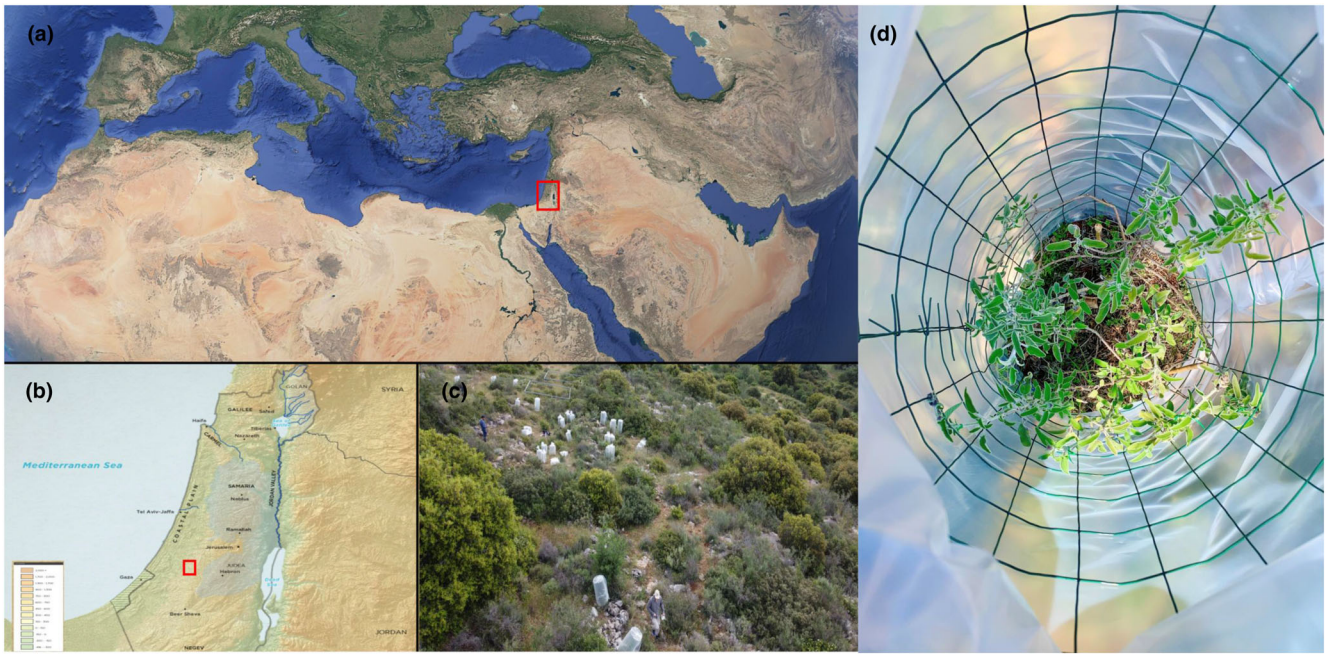

Fig. 1 Study site and experimental setup. (a) Regional map of the Eastern Mediterranean. (b) Location of the field site in the Judean foothills, Israel. (c) Natural plot with protective enclosures around selected plants. (d) Overhead view of *Salvia fruticosa* inside a dust-exposure structure.

Zhang *et al.*, 2015), as shown in Table S4. Natural dust events are variable in composition, difficult to replicate, and often insufficient in quantity for large-scale field application experiments. The use of a naturally occurring dust analog provided a consistent, uncontaminated source free from atmospheric processing and industrial pollutants encountered during long-range transport. To produce the dust analog, we followed common procedures described previously (Stockdale *et al.*, 2016; Gross *et al.*, 2021; Starr *et al.*, 2023; Lokshin *et al.*, 2025). The dust was generated from surface soils collected near the upper cable car station of Mount Etna, Italy (37°42′N, 14°60′E), and processed through a setup of sieves to achieve a particle size smaller than 63 µm (size subjected to wind erosion). The mineralogical composition of the dust was determined using X-ray powder diffraction with a Panalytical Empyrean diffractometer and analyzed via MATCH! software with the PDF-2 library. Elemental composition was analyzed by X-ray fluorescence using a Panalytical Axios spectrometer equipped with a rhodium anode X-ray tube and multiple analyzing crystals. Elemental concentrations were determined by an ICP-MS Agilent 8900cx at the Hebrew University of Jerusalem following a concentrated acid extraction procedure (Lokshin *et al.*, 2024a, 2025).

Experimental design

The experiment was conducted over 3 months, from February 3 to April 25, 2025, coinciding with the main dust season in the region, with March typically experiencing the highest dust deposition (Ganor & Foner, 2001; Ganor *et al.*, 2010). Each of the three selected plant species (*C. creticus*, *S. fruticosa*, and *T. capitatum*) was represented by 12 individual plants ($n = 36$), with six receiving dust applications directly on their foliage ('foliar dust application treatment') and six serving as untreated controls. To assess the potential for root-mediated uptake, an additional 12 individuals of *C. creticus* were included, with six receiving dust applications directly to the soil surface near their roots ('root application treatment'), and six serving as controls, yielding a total of 48 experimental plants.

On the first day of the experiment, before the first dust application, protective structures were installed around all plants, including both dust-treated and control groups, to ensure identical exposure to microenvironmental conditions and to minimize disturbances from wind, rain, and wildlife. Each enclosure was a 40 cm diameter, 80 cm high cylinder of flexible skeletal fencing wrapped in transparent agricultural film, permeable to sunlight and left open at the lower 20 cm to allow air circulation (Fig. 1). The design allowed for good light penetration and airflow, and no differences in plant appearance or condition were observed between control and dust-treated plants that could be attributed to the enclosures. Since most of the dust deposition occurs in a limited number of dust storm days from the Sahara (Ganor *et al.*, 2010), dust was applied in three pulses, on February 5, March 1, and March 30, timed to coincide with peak regional dust storm activity and designed to mimic natural seasonal deposition (Ganor & Foner, 2001; Gross *et al.*, 2021; Lokshin *et al.*, 2025). Application rates were based on documented regional dust deposition and standardized to 30 $g\,m^{-2}$ per pulse, which represents the monthly deposition in March (Ganor & Foner, 2001; Dayan *et al.*, 2008). Based on plant-specific leaf area estimates for each species, which were determined in parallel trials, the corresponding total application in the foliar dust application treatment was adjusted for the specific canopy area of each

© 2026 The Author(s).
New Phytologist © 2026 New Phytologist Foundation.

14698137, 0, Downloaded from https://nph.onlinelibrary.wiley.com/doi/10.1111/nph.71112 by CochraneAustria, Wiley Online Library on [08/04/2026]. See the Terms and Conditions (https://onlinelibrary.wiley.com/terms-and-conditions) on Wiley Online Library for rules of use; OA articles are governed by the applicable Creative Commons License

14698137, 0, Downloaded from https://nph.onlinelibrary.wiley.com/doi/10.1111/nph.71112 by CochraneAustria, Wiley Online Library on [08/04/2026]. See the Terms and Conditions (https://onlinelibrary.wiley.com/terms-and-conditions) on Wiley Online Library for rules of use; OA articles are governed by the applicable Creative Commons License

plant (Gross *et al.*, 2021; Lokshin *et al.*, 2025). Larger individuals received 2–3 g of dust per pulse, while smaller individuals received *c.* 2 g per pulse, resulting in a total application per plant of 6–9 g (Table S5). Over the course of the experiment, a small portion of the material applied to the leaves naturally fell from the leaf surfaces to the underlying soil due to environmental factors such as gravity and wind. The root application treatment group of *C. creticus* received a single pulse of 6 g dust application, concurrent with the foliar application treatment. To track the effects of dust on plant development and growth, four branches were tagged on each plant before the first dust application, enabling repeated growth measurements throughout the experiment (Holzapfel *et al.*, 2006).

Soil analyses, plant growth, and elemental analysis

After 3 months of dust exposure, the experiment was terminated. Before the plants were harvested, growth and biomass parameters were recorded for all individuals. These included average branch length, number of leaves per tagged branch, and the relative biomass of the tagged branches, adjusted for each plant's size (Figs S3, S4). Afterward, the plants were harvested, separated into roots and shoots, and taken to the lab for further analysis. The tagged branches used for growth measurements were returned to their original plants before harvesting. The plants were thoroughly washed with 0.1 M HCl, followed by three rinses with deionized water to remove externally adhered particles to minimize contamination (Gross *et al.*, 2021; Lokshin *et al.*, 2024b, 2025). Shoots and roots were dried at 60°C, weighed for biomass determination, and ground into fine powder. Samples were then ashed at 550°C for 4 h and digested in 1 M HNO_3. Roots and shoots' elemental composition was determined using an ICP-MS Agilent 8900cx at the Hebrew University of Jerusalem.

Soil samples were collected from beneath each of the studied plants to assess nutrient availability, pH, and elemental composition in order to monitor the impact of dust deposition on soil geochemistry (Fig. S5). Acid-extractable nutrient pools were determined by extracting 0.5 g of soil with 20 ml of 1 M HNO_3 for 1 h at room temperature, followed by shaking, centrifugation, and ICP-MS analysis (Lokshin *et al.*, 2025). This acid extraction targets acid-labile nutrients from primary minerals (e.g. apatite) and Fe/Mn oxides, representing a reservoir that can become available over longer timescales, as shown by (Nezat *et al.*, 2007).

To rule out contamination from residual dust particles on leaf surfaces, we modeled a worst-case scenario assuming 10% of the applied dust remained adhered to the shoots of *C. creticus*, *S. fruticosa*, and *T. capitatum*. Based on measured elemental concentrations in both dust and plant digests, we calculated the predicted nutrient content if passive contamination (without uptake) had occurred. Actual leaf retention was not measured in our study, and the 10% value is an assumed estimate; field-derived retention data from Uni & Katra (2017) who measured dust deposition on foliage during natural dust events, reported values ranging between 8.1 and 9.2 g m^{-2}, which, depending on dust loading and leaf area, broadly supports our assumption. Controlled laboratory studies by Gross *et al.* (2021) and Golan *et al.* (2025) further examined leaf retention under experimental conditions, providing complementary evidence for the plausibility of our estimate. For instance, in *C. creticus*, 0.7 g of residual dust on a 23 g shoot equates to *c.* 3% of the sample mass. Predicted concentrations for Fe, Mn, Cu, and Ni were compared to measured values in dust-treated plants. Observed concentrations substantially exceeded predictions and deviated from expected dust-plant mixing lines (Fig. S6a), supporting active uptake.

REE analysis further supported this interpretation (Fig. S6b). Most REEs, including La, Ce, Nd, Sm, and Gd, were enriched beyond contamination-based expectations. This pattern suggests selective uptake and fractionation during foliar assimilation. Together, these results confirm that nutrient enrichment reflects biologically mediated foliar uptake rather than passive surface contamination.

Rare earth element (REE) tracing

The REEs are a group of trace metals comprising the lanthanide series (atomic numbers 57–71) that exhibit similar, though not identical, chemical properties. These characteristics make REEs widely used as tracers in geosciences, environmental, and biological studies (Elderfield *et al.*, 1988; Liang *et al.*, 2008), and for mineral dust source tracing specifically (Laveuf & Cornu, 2009; Palchan *et al.*, 2018; Guinoiseau *et al.*, 2022). Particularly, the unique heavy-to-light REE ratios of volcanic dust can be used to differentiate between soil and dust-derived inputs in plants (Censi *et al.*, 2017; Yusupov *et al.*, 2020) and provide a tool for tracing dust-borne nutrient fluxes. REE concentrations were measured in all 48 plant samples using inductively coupled plasma mass spectrometry (ICP-MS) following closed-vessel acid digestion with concentrated HNO_3 and HCl. Elemental concentrations were normalized to CI-chondrite values (Barrat *et al.*, 2012), enabling comparison of REE distribution patterns across samples and detection of source-specific signatures. The raw (non-normalized) REE concentrations are provided (Tables S4, S6). La : Lu ratios were calculated to assess light-to-heavy REE fractionation, a sensitive indicator of differences between dust and soil sources. The REE composition of the local Terra Rossa soil was based on published values (Palchan *et al.*, 2018). In this system, volcanic dust and local soils exhibit distinct REE patterns and light REE-enriched (LREE)/HREE distributions, supporting their use as geochemical tracers of nutrient origin (Lokshin *et al.*, 2024a).

Leaf surface pH and organic acids

Leaf surface pH was measured using a portable flat-surface pH electrode (HI-1413; HANNA Instruments, Woonsocket, RI, USA) on five leaves per plant across treatments (Golan *et al.*, 2025; Lokshin *et al.*, 2025). For organic acid analysis, *c.* 10 g of fresh leaves was manually shaken with 10 ml of deionized water and 10 ml of methanol for 10 min to extract surface metabolites (Gross *et al.*, 2021; Golan *et al.*, 2025). Extracts were filtered and spiked with 50 µl of ribitol (0.2 mg ml^{-1}), used as an internal standard due to its absence in plant tissues. Extracts were

© 2026 The Author(s).
New Phytologist © 2026 New Phytologist Foundation.

14698137, 0, Downloaded from https://nph.onlinelibrary.wiley.com/doi/10.1111/nph.71112 by CochraneAustria, Wiley Online Library on [08/04/2026]. See the Terms and Conditions (https://onlinelibrary.wiley.com/terms-and-conditions) on Wiley Online Library for rules of use; OA articles are governed by the applicable Creative Commons License

then stored at −80°C until analysis. Before analysis, samples were vacuum-dried overnight to eliminate residual solvents that could interfere with derivatization. Dried residues were resuspended in 40 µl of methoxamine hydrochloride (20 mg ml^{-1} in pyridine) and incubated at 37°C for 90 min to stabilize carbonyl groups. Then, 70 µl of MSTFA (N-methyl-N-(trimethylsilyl) trifluoroacetamide) was added and incubated at 37°C for 30 min to silylate hydroxyl, carboxyl, and amine groups, rendering them volatile and suitable for gas chromatography. One microliter of derivatized extract was injected in splitless mode into a GC-MS system (Agilent 7890A GC coupled to a 5975C mass selective detector), using helium as carrier gas (0.6 ml min^{-1}) and an HP-5MS capillary column (30 m × 0.25 mm × 0.25 µm). Mass spectra were recorded at *m/z* 50–550 and analyzed using MassHunter software. Metabolites were identified using certified plant standards (Sigma-Aldrich) and the NIST 14 MS spectral library. A six-point 2-fold serial dilution calibration curve of ribitol (starting at 0.05 mg ml^{-1}) was used to validate quantification. Organic acid abundances were normalized to ribitol and expressed as relative peak area or µg per gram fresh leaf weight. The analysis focused on acids known to enhance macro- and micronutrient solubility, including malic and citric acids (Yoshida *et al.*, 1997; Tiwari *et al.*, 2022). This two-step derivatization method (methoximation followed by sialylation) is widely used for the comprehensive profiling of plant-derived polar metabolites (Gross *et al.*, 2021).

Leaf surface and rhizosphere microenvironment simulation experiments

An artificial solution was prepared to simulate the leaf surfaces and the rhizosphere microenvironments. The solution was made from a potassium phosphate buffer adjusted to pH 6, the average pH of the leaf surfaces of the three plant species in our study (Fig. 4a) and chosen to approximate the localized acidification that can occur in rhizosphere zones even within alkaline soils (Lindsay & Norvell, 1978; Jones, 1998). The buffer solution contained oxalic, malic, and citric acids, which are present in the leaf surfaces of the studied plants (0.005 M each, 1 : 1 : 1 ratio) (Yoshida *et al.*, 1997; Tiwari *et al.*, 2022) and in a typical rhizosphere (Jones, 1998). For the leaf surface simulation, two replicate samples of 0.5 g of dust were placed onto an artificial polyethylene leaf-like surface (0.1 m by 0.1 m). Then, 2 ml of the artificial solution was uniformly sprinkled on the dust to achieve a solid-to-liquid ratio of 1 : 4, which resembles natural leaf surface exudation volume. To simulate evaporation from the leaf surface, the samples were incubated at 25°C to continuously evaporate the solution until completely dry (*c.* 3 d). The application and evaporation cycle were repeated twice. After 1 wk, the dust was rinsed from the artificial surface with 10 ml of double-distilled water (DDW), centrifuged, and the supernatant analyzed using ICP-MS. The exact same experimental setup was performed with DDW instead of the leaf solution, as a control. The rhizosphere microenvironment simulation experiments represent dust dissolution in soil, where the ratio of exudation volume to dust mass is much lower than on the leaf surface. Two replicate samples of 5 g of soil collected from the study site were placed in 50 ml tubes and amended with 0.5 g of dust. The dust-to-soil ratio (10%) represents an extreme case of dust deposition at the site (*c.* 0.01–0.1% of soil mass), chosen to maximize the potential dissolution signal under experimental conditions. While higher than natural loading, this ratio allows for a clear comparison with the leaf surface scenario, and the qualitative contrast between leaf and root uptake pathways is expected to hold at lower, more typical dust deposition rates. Then, the soil-dust mixture was injected with 4 ml of artificial solution, matching that used for the leaf surface simulation, using a syringe to simulate root exudation. This volume was selected to reflect typical differences in moisture availability and exudation volumes between the rhizosphere and leaf surface, where root environments maintain higher water content, in contrast to the limited, thin moisture films present on leaves (Yoshida *et al.*, 1997; Smith, 2007). The soils were incubated for 1 wk under the same conditions as the leaf surface experiment, with a second injection after 3 d, mirroring the leaf simulation protocol. In parallel, two additional soil-only samples (5 g each) were injected with 4 ml of the artificial solution to assess its effect on background soil nutrient levels in the absence of dust. In addition, control treatments included four soil-only and soil-plus-dust samples that received DDW instead of the artificial solution. Nutrient solubility was compared between the artificial leaf surface or rhizosphere solutions and the DDW controls. In the rhizosphere experiment, the initial soil nutrient solubility subjected to the rhizosphere artificial solution (the soil-only experiment) was subtracted from that of the soil plus dust treatment.

Global geospatial analysis of dust nutrient contributions to plants

A global geospatial analysis was conducted to quantify the nutritional contribution of dust inputs to vegetation world-wide and identify high-dust-impact regions. The analysis combines field-derived measurements of dust nutrient uptake fractions with published data of global dust deposition, source-region elemental composition, and global soil bioavailable nutrient fluxes (Paytan *et al.*, 2009; Zhang *et al.*, 2015; Kok *et al.*, 2021). All geospatial analyses were performed using QGIS (v.3.16.15), and final global maps were rendered at a spatial resolution of 1.875° latitude × 2.5° longitude.

Estimation of dust-borne nutrient uptake fractions from the field experiment

The fraction of nutrients in dust that are available for plant uptake was derived from our field experiment data. For Fe, Mn, and Cu, we calculated species-averaged changes in shoot tissue concentration (µg g^{-1}) following foliar dust application, relative to untreated controls. These values were used to estimate the efficiency of uptake, which is the proportion of each nutrient that was taken up by plants relative to its total concentration per gram of deposited dust (Table S5). To calculate the uptake efficiency, the following equations were used:

© 2026 The Author(s).
New Phytologist © 2026 New Phytologist Foundation.

$$\Delta C_X = C_{X,treated} - C_{X,control} \left(\mu g\ g^{-1}\right) \quad \text{Eqn 1}$$

ΔC_X = net increase in the concentration of element X due to dust application, $C_{X,treated}$ = concentration of element X in treated plants, $C_{X,control}$ = concentration of element X in control plants.

$$U_X = \Delta C_X \times m_{leaf}\ (g) \quad \text{Eqn 2}$$

U_X = total amount of nutrient X taken up, m_{leaf} = dry mass of aboveground biomass (g).

$$A_X = m_{dust} \times f_{x,dust}\ (mg) \quad \text{Eqn 3}$$

A_X = total amount of nutrient X present in the applied dust, m_{dust} = mass of dust applied per plant (g), $f_{x,dust}$ = concentration of element X in the dust used in this study ($mg\ g^{-1}$ or %) (Table S4).

$$F_{X,plant} = \frac{U_X}{A_X} \quad \text{Eqn 4}$$

$F_{X,plant}$ = fraction of nutrient X taken up by the plant.P posed a unique challenge due to its high mobility and rapid redistribution within plant tissues (Fernández & Brown, 2013; Page & Feller, 2015), which limited the detection of consistent concentration changes in the field. As a result, the uptake efficiency for P was based on measurements from a previous glasshouse experiment on P-deficient crop plants (Lokshin *et al.*, 2025), yielding a conservative estimate of 8.33%.

Annual deposition fluxes

The uptake efficiencies ($F_{X,plant}$, Eqn 4) were applied globally to compute spatially resolved fluxes of plant-available P, Fe, Mn, and Cu from dust deposition ($mg\ m^{-2}\ yr^{-1}$), using a grid resolution of 1.875° latitude × 2.5° longitude. Global annual dust deposition rates were derived from an ensemble model (Kok *et al.*, 2021), and regional dust nutrient concentrations were based on source-specific measurements (Paytan *et al.*, 2009; Zhang *et al.*, 2015). To calculate the annual nutrient deposition fluxes, we used the following equations:

$$D_X = D_{dust} \times f_{x,dustZ} \quad \text{Eqn 5}$$

D_X = annual total deposition flux of nutrient X ($mg\ m^{-2}\ yr^{-1}$); D_{dust} = annual dust deposition flux ($g\ m^{-2}\ yr^{-1}$) derived from (Kok *et al.*, 2021); $f_{X,dustZ}$ = the average concentration of nutrient X in dust ($mg\ g^{-1}$), taken from (Zhang *et al.*, 2015) for Fe, Mn, and P, and from (Paytan *et al.*, 2009) for Cu.

This deposition flux was multiplied by the experimentally derived plant uptake efficiency to obtain the bioavailable fraction:

$$F_{X,bioD} = D_X \times F_{X,plant} \quad \text{Eqn 6}$$

$F_{X,bioD}$ = annual bioavailable flux of nutrient X from dust ($mg\ m^{-2}\ yr^{-1}$).

Comparison with soil nutrient fluxes

To evaluate the relative contribution of dust-derived nutrient deposition to the vegetation, plant-available dust nutrient fluxes were compared with bioavailable nutrient fluxes from soils on an annual basis, using the global dataset compiled by (Ochoa-Hueso *et al.*, 2023). This dataset reports bioavailable fluxes of Fe, Mn, Cu, and P from ion-exchange membrane deployments across a large number of plots world-wide, covering a wide range of ecosystems. We focused only on untreated, non-agricultural plots, resulting in a total of 133 plots world-wide (Fig. S7). Nutrient flux values, based on a mean membrane exposure time of 58 d, were scaled to annual rates by multiplying by 6.88 (365 ÷ 58). The contribution of annual nutrient deposition from dust relative to soil fluxes was computed for each grid cell only in regions where soil nutrient flux data were available, as:

$$R_X = \frac{F_{X,bioD}}{S_X} \quad \text{Eqn 7}$$

R_X = ratio of dust-derived flux to soil-derived flux of nutrient X, S_X = annual soil-derived bioavailable flux of nutrient X ($mg\ m^{-2}\ yr^{-1}$).

Soil nutrient flux data were spatially matched to the dust model grid using a nearest-neighbor approach. At each site (where soil nutrient fluxes were available, Fig. S7), the ratio of dust-to-soil nutrient fluxes (R_X, Eqn 7) was calculated by dividing the modeled dust-derived bioavailable flux by the corresponding annual soil-nutrient-derived flux, enabling a direct comparison of dust and soil contributions to plant nutrition.

Atmospheric nutrient contribution per dust event

Nutrient inputs from atmospheric dust occur in sporadic, high-intensity deposition events, whereas soil nutrient fluxes are more continuous, driven by slower biogeochemical processes. To enable a realistic comparison between these pulse-driven fluxes and daily soil nutrient fluxes, we normalized the modeled annual dust nutrient fluxes to individual dust events and compared them to the average daily nutrient supply from soils. The analysis was focused on the Mediterranean region only. The number of annual dust deposition days (N_{dust}) was assumed to be 28 based on long-term observations in the region (Ganor *et al.*, 2010). Soil nutrient fluxes were averaged over 365 d.

The per-event (dust-day) nutrient flux was calculated as:

$$R_{X,daily} = \frac{F_{X,bioD}/N_{dust\ days}}{S_X/365} \quad \text{Eqn 8}$$

$R_{X,daily}$ = ratio of daily dust-derived flux to the soil-derived flux of nutrient X; $N_{dust\ days}$ = Number of dust deposition days per year (assumed 28).

Due to limited Mediterranean soil flux data, which was restricted to two reference sites in Spain (Ochoa-Hueso *et al.*, 2023), soil nutrient fluxes were extrapolated across the Mediterranean climate zone (Peel *et al.*, 2007). This

© 2026 The Author(s).
New Phytologist © 2026 New Phytologist Foundation.

14698137, 0, Downloaded from https://nph.onlinelibrary.wiley.com/doi/10.1111/nph.71112 by CochraneAustria, Wiley Online Library on [08/04/2026]. See the Terms and Conditions (https://onlinelibrary.wiley.com/terms-and-conditions) on Wiley Online Library for rules of use; OA articles are governed by the applicable Creative Commons License

14698137, 0, Downloaded from https://nph.onlinelibrary.wiley.com/doi/10.1111/nph.71112 by CochraneAustria, Wiley Online Library on [08/04/2026]. See the Terms and Conditions (https://onlinelibrary.wiley.com/terms-and-conditions) on Wiley Online Library for rules of use; OA articles are governed by the applicable Creative Commons License

extrapolation was supported by measurements from other Mediterranean sites (Rashid & Ryan, 2004; Navarro-Pedreño *et al.*, 2018; Moreno-Jiménez *et al.*, 2019) and by our own site-level measurements (Table S2), all showing similar nutrient concentrations.

Uncertainty estimation

To explore variability in our global nutrient flux model, we performed a bounding uncertainty analysis, applying ±1 SD to each input variable to estimate the upper and lower limits of possible outcomes. This approach provides a possible range of extremes rather than a probabilistic confidence interval. These extremes do not correspond to statistical confidence intervals or probability of occurrence. Dust deposition uncertainties (±1 SD) were taken from (Kok *et al.*, 2021). To represent natural variation in nutrient uptake, we used SD values from replicate plants ($n = 18$) in the field experiment (Table S5), which reflect variability between plant species, traits such as plant size, dust retention capacity on leaves, microenvironmental conditions, health, and growth stage of each individual plant. Dust elemental concentrations of P, Fe, and Mn were taken from (Zhang *et al.*, 2015), which compiled data from multiple studies. Due to inconsistent reporting, SD values for these elements were not systematically available, and concentrations were treated as fixed inputs. The same applies to Cu, which was based on (Paytan *et al.*, 2009). Gridded global estimates of bioavailable nutrient fluxes, along with their upper and lower bounds based on the bounding uncertainty analysis in model inputs, as described above, are provided in the supplementary data files.

Statistical analysis

All statistical analyses were performed using GraphPad Prism v.10.0.1 (GraphPad Software, San Diego, CA, USA) and custom scripts in Python. Treatment effects on foliar elemental concentrations and plant biomass were evaluated using one-way ANOVA followed by Tukey's multiple comparisons test ($\alpha = 0.05$). Principal component analysis was applied to rare earth element (REE)profiles to distinguish between foliar uptake and external surface contamination. Linear regression was used to examine relationships between dust-induced biomass responses, elemental enrichment in foliage, and background soil nutrient availability. To minimize spatial autocorrelation and avoid pseudo-replication, plants were randomly assigned to treatments and interspersed within plots, ensuring that treated and control individuals experienced comparable microsite conditions and could be considered independent replicates.

Results

In situ foliar dust uptake

Foliar dust application significantly increased shoot micronutrient concentrations across all three species (Fig. 2a), with mean dust-to-control fold increases averaged across species of 4.02 for Fe, 1.88 for Mn, 3.3 for Ni, and 1.47 for Cu. A moderate increase in Mg (1.32-fold) was also observed in *S. fruticosa* (Fig. S1). Nutrient enrichment was confined to shoots; root concentrations remained mostly unchanged across all species (Fig. S2). To assess the role of dust-borne nutrient uptake from roots, we applied dust directly to the soil near the roots of *C. creticus* in a separate treatment. Only modest (but significant) increases in shoot Fe and Ni were observed (Fig. 2b), suggesting limited root-mediated uptake.

Tracing dust nutrient uptake using rare earth elements analyses

Rare earth elements can serve as geochemical tracers for nutrient sources due to their low background levels in plant tissues and their characteristic source-specific patterns (Yusupov *et al.*, 2020; see the Materials and Methods section). Concurrently with the observed increases in nutrients, plants that received foliar dust applications showed a clear and significant increase compared to controls (Fig. 3a), with consistent shifts from soil-like to dust-like REE patterns across all three species (Fig. 3b,c). Given the source-specific signatures of REEs and their low natural abundance in plant tissues, the shift from soil-like to dust-like patterns supports foliar uptake of dust-borne elements. By contrast, root-applied dust in *C. creticus* led to a modest (yet significant) increase in total REE concentration in shoot tissue, substantially lower than that observed in foliar-applied plants, further underscoring the importance of the foliar uptake pathway. Lanthanum-to-lutetium (La : Lu) ratios in foliar-dusted plants were markedly elevated compared with the control plants and shifted toward the value of the applied dust, where the control plants show only a slight elevation from the value of the local soils (Fig. 3b). The signature in the control plants is slightly elevated from the soil due to a minor fractionation (Liang *et al.*, 2008), but the signature in the foliar-dusted plants is significantly elevated both from the soils and from the control plants, suggesting foliar dust contribution to plants. By contrast, root-applied plants caused no change in their La : Lu ratios, further supporting the dominance of direct foliar uptake. While La : Lu ratios in foliar-dusted plants approached those of the dust itself, they remained slightly lower, likely due to the mixing of two sources – the local soils and applied dust. Furthermore, the REE pattern of foliar-dusted plants also shows a LREE profile that mirrors the applied dust source, while the control plants align more closely with the soil composition (Fig. 3c), indicating a clear foliar uptake contribution, corroborating a previous study using radiogenic neodymium isotope tracing (Lokshin *et al.*, 2025).

Mechanism of foliar nutrient uptake from dust

All three species we studied exhibited mildly acidic leaf surfaces, with mean pH values near 6, substantially lower than the surrounding alkaline soil (Fig. 4a). Malic and citric acids were detected on leaf surfaces across all species (Table S3). In a controlled incubation experiment, we mimicked dust interaction

© 2026 The Author(s).
New Phytologist © 2026 New Phytologist Foundation.

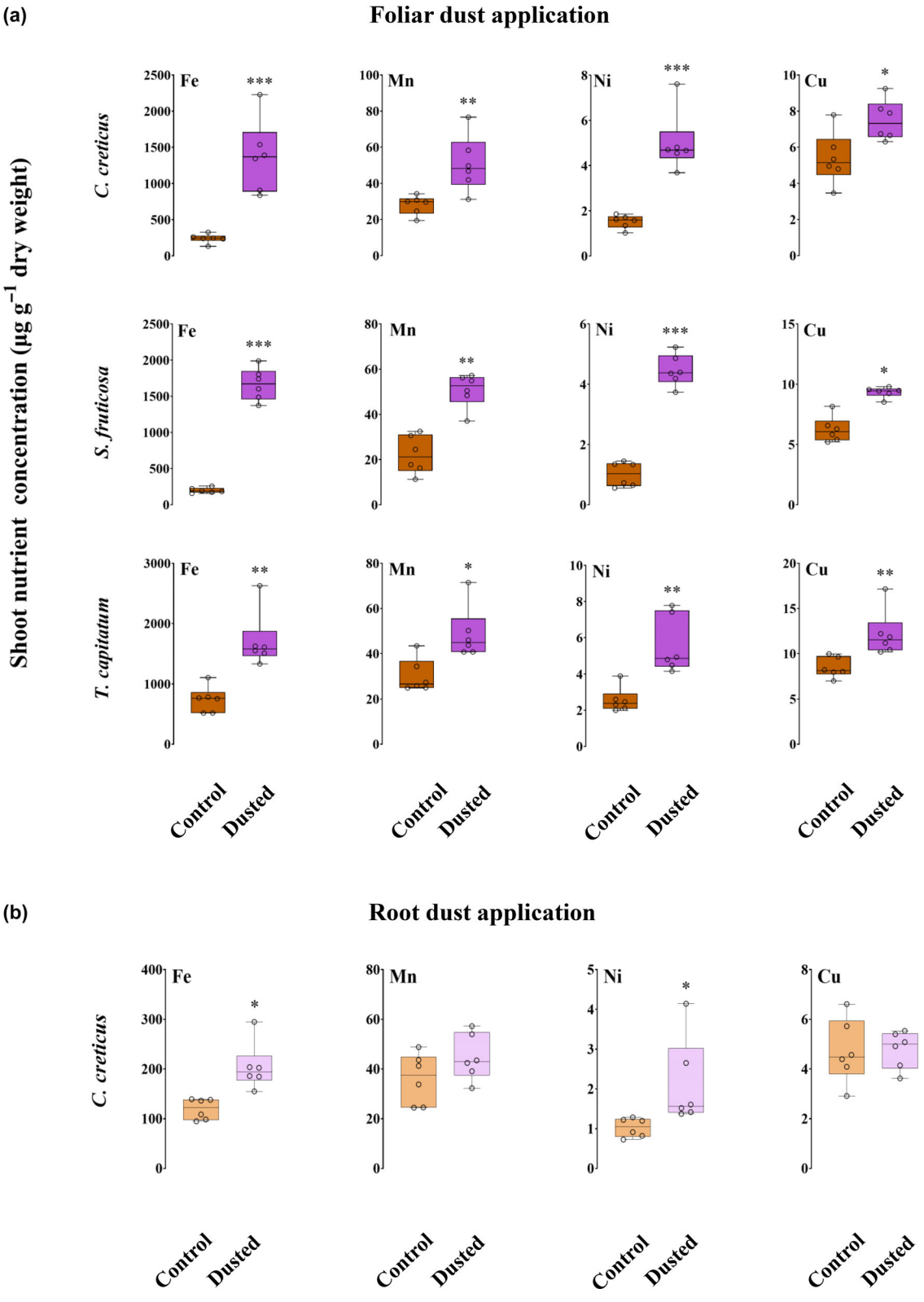

Fig. 2 Foliar and root uptake of micronutrients from dust in Mediterranean shrub species. (a) Concentrations of Fe, Mn, Ni, and Cu in the shoots of *Cistus creticus*, *Salvia fruticosa*, and *Teucrium capitatum* following foliar application of mineral dust in three monthly pulses (February to April). Control plants are shown in brown; dust-treated plants are in purple. (b) Shoot concentrations of the same micronutrients in *C. creticus* after root application of mineral dust. Control plants are shown in pale brown; dust-treated plants in pale purple. Data are presented as boxplots with individual biological replicates ($n = 6$ plants per treatment). Asterisks denote statistically significant differences relative to controls (*, $P < 0.05$; **, $P < 0.01$; ***, $P < 0.001$; two-sided *t*-test).

© 2026 The Author(s).
New Phytologist © 2026 New Phytologist Foundation.

14698137, 0, Downloaded from https://nph.onlinelibrary.wiley.com/doi/10.1111/nph.71112 by CochraneAustria, Wiley Online Library on [08/04/2026]. See the Terms and Conditions (https://onlinelibrary.wiley.com/terms-and-conditions) on Wiley Online Library for rules of use; OA articles are governed by the applicable Creative Commons License

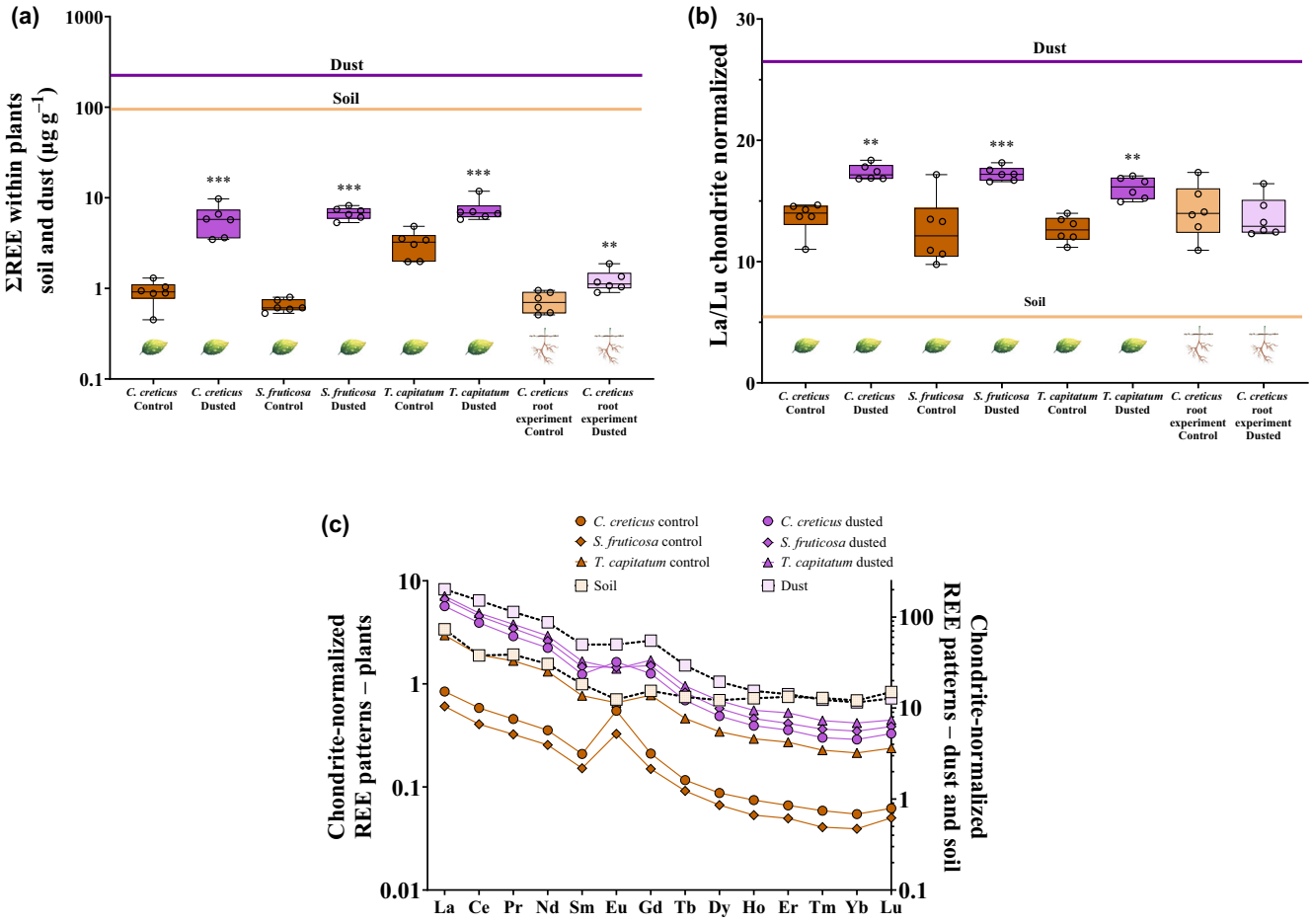

Fig. 3 Rare earth element (REE) signatures in dust, soil, and plants. (a) Total REE concentrations (ΣREE) in shoot tissue of *Cistus creticus*, *Salvia fruticosa*, and *Teucrium capitatum* following foliar dust application (purple) or in control plants (brown). Purple and brown lines represent dust and soil values, respectively. An additional root application treatment experiment for *C. creticus* is shown on the right (light colors). (b) Chondrite-normalized La : Lu ratios in the same plants and treatments. The purple line represents the dust value, and the brown line represents the soil value. (c) Chondrite-normalized REE patterns in shoot tissue following foliar dust application (purple) and controls (brown) compared to the applied dust (light purple) and local soil (light brown) (Palchan *et al*., 2018). Plant values are averaged per treatment and plotted against the left *y*-axis; dust and soil values are plotted on the right *y*-axis. Each boxplot shows the median, interquartile range, and individual values ($n = 6$ per plant treatment; $n = 6$ for soil; $n = 2$ for dust). Asterisks indicate significant differences relative to the corresponding control (**, $P < 0.01$; ***, $P < 0.001$; one-way ANOVA with Tukey's *post hoc* test).

with the leaf surface microenvironment by exposing mineral dust to an artificial leaf surface solution that mirrors the chemical composition of the studied plants, embedded on a leaf-like structure. The artificial leaf surface solution increased the dissolution of dust Fe, Mn, Zn, Mg, Ni, and Cu by several orders of magnitude in comparison to dissolution in water. By contrast, exposing dust to the soil root zone microenvironment by injecting an artificial solution of a typical rhizosphere to dust-amended soil from the study site yielded significantly lower dissolution in comparison to the leaf simulation (Fig. 4b). These results suggest that the unique chemical environment of leaf surfaces plays a key role in mobilizing otherwise poorly soluble nutrients from atmospheric dust, driven by the relatively high ratios of dust mass-to-leaf solution volumes. We attribute the reduced nutrient solubility in the rhizosphere simulation to the lower ratios of dust mass-to-soil volume and to secondary chemical interactions with soil minerals.

Global spatial analysis of dust contribution to plant nutrition

The experimentally determined foliar uptake fractions of dust-borne micronutrients (Fe, Mn, Cu) were combined with global dust deposition fluxes (Kok *et al*., 2021) and total dust elemental concentrations from major source regions (Zhang *et al*., 2015) to estimate the world-wide contribution of dust to plant nutrition and identify regions where dust supplies a significant flux of bioavailable nutrients to vegetation. For P, the uptake fraction from dust was derived from previous glasshouse experiments rather than the current field study (Lokshin *et al*., 2025; see the Materials and Methods section). We calculate the annual deposition of plant-available Fe and P to reach up to 17 mg m^{-2} yr^{-1}, while Cu and Mn amounts up to 0.1 mg m^{-2} yr^{-1} (Fig. 5). The highest fluxes emerged near major dust source regions in Africa, the Mediterranean, the

© 2026 The Author(s).
New Phytologist © 2026 New Phytologist Foundation.

14698137, 0, Downloaded from https://nph.onlinelibrary.wiley.com/doi/10.1111/nph.71112 by CochraneAustria, Wiley Online Library on [08/04/2026]. See the Terms and Conditions (https://onlinelibrary.wiley.com/terms-and-conditions) on Wiley Online Library for rules of use; OA articles are governed by the applicable Creative Commons License

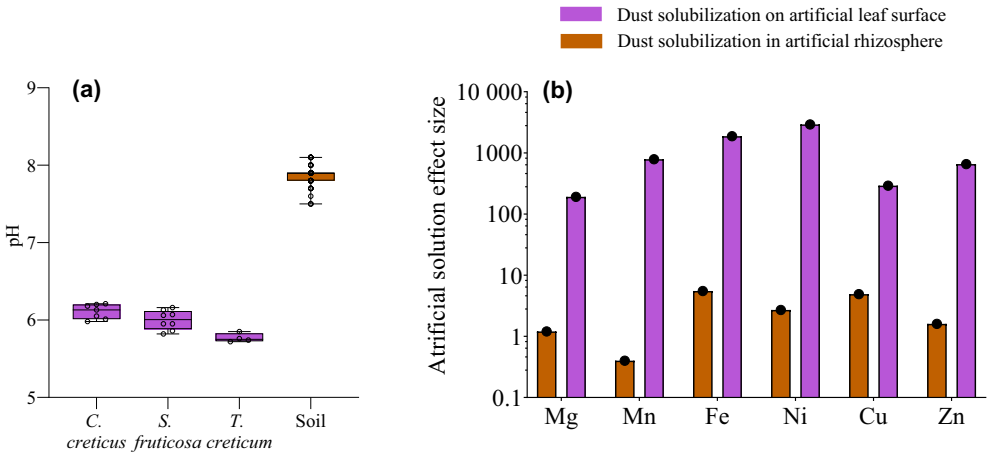

Fig. 4 Dust nutrient solubilization in artificial leaf and rhizosphere microenvironments. (a) pH of leaf surfaces of *Cistus creticus*, *Salvia fruticosa*, and *Teucrium capitatum*, and of soil from the study site ($n = 9$–10 per group). (b) Effect size of dust solubilization for Mg, Mn, Fe, Ni, Cu, and Zn in artificial leaf surface (purple) and rhizosphere (brown) solutions in comparison to solubilization in deionized water; values are shown on a logarithmic scale ($n = 2$).

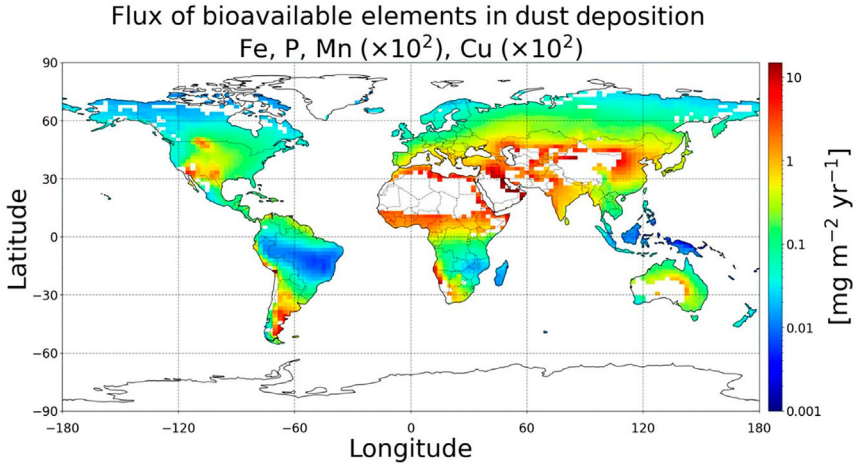

Fig. 5 Annual deposition fluxes of bioavailable Fe, P, Mn, and Cu. Global map showing annual deposition fluxes of bioavailable Fe, P, Mn, and Cu (mg m^{-2} yr^{-1}). Bioavailable fractions for Fe, Mn, and Cu are based on measured data from the field experiment, and for P from a glasshouse experiment (Lokshin *et al.*, 2025). Mn and Cu values are scaled by a factor of 100 (×10^2), as indicated in the title. White areas represent regions excluded from the analysis.

Western United States and Central and Eastern Asia. Non-vegetated areas were excluded from the analysis using the Köppen climate classification by masking regions lacking persistent vegetation cover, including deserts, tundra, and ice-covered zones (i.e. BWh, BWk, ET, and EF classes; Peel *et al.*, 2007). These spatial estimates highlight regions where foliar uptake of dust-borne nutrients may constitute a substantial component of plant nutrient supply under current deposition patterns. While these geographic patterns highlight the potential scale of the process, actual uptake efficiency will depend on plant and environment-specific factors. We compared the annual contribution of dust-derived micronutrients to vegetation relative to soil bioavailable nutrient fluxes in world-wide locations (Ochoa-Hueso *et al.*, 2023) and identified two hotspots of high contribution (up to 17% annually for Fe, and smaller extent for Mn and Cu, Fig. 6a,c,d): the Mediterranean region and the Western United States, both situated in areas of high dust deposition. For P, a notable hotspot of annual dust contribution appears in the Eastern Amazon rainforest (up to 12% annually, Fig. 6b) supplied by *Trans*-Atlantic Saharan dust (Bristow *et al.*, 2010; Gross *et al.*, 2016), which compensates for exceptionally low soil P bioavailability in that region (Van Langenhove *et al.*, 2020).

Discussion

This study provides the first experimental evidence that dust deposition can substantially support plant nutrition via direct foliar uptake, a trait potentially prevalent across many plant species. The actual uptake efficiency is likely influenced by plant-specific traits such as trichome density, cuticular composition, and stomatal distribution, as well as by vegetation type and local climatic conditions (e.g. humidity and rainfall). Recent studies have shown considerable interspecific variation in foliar nutrient uptake across both crop species and trees, highlighting the importance of such trait-based variation (Gross *et al.*, 2021; Starr *et al.*, 2023). Incorporating targeted experiments across diverse ecological zones will be essential for refining global estimates of dust-derived foliar nutrient acquisition. Atmospheric processes during dust transport, such as acid exposure, photochemical alteration, and wet deposition via rain or fog, can enhance nutrient solubility and uptake (Stockdale *et al.*, 2016; Li *et al.*, 2017; Mahowald *et al.*, 2018; Baker *et al.*, 2021; Dam *et al.*, 2021). Similarly, non-rainfall moisture inputs such as dew may act as important facilitators of foliar nutrient uptake (Matos *et al.*, 2022), as the temporarily available moisture promotes both dust retention and nutrient dissolution. Dewfall is common in

© 2026 The Author(s).
New Phytologist © 2026 New Phytologist Foundation.

14698137, 0, Downloaded from https://nph.onlinelibrary.wiley.com/doi/10.1111/nph.71112 by CochraneAustria, Wiley Online Library on [08/04/2026]. See the Terms and Conditions (https://onlinelibrary.wiley.com/terms-and-conditions) on Wiley Online Library for rules of use; OA articles are governed by the applicable Creative Commons License

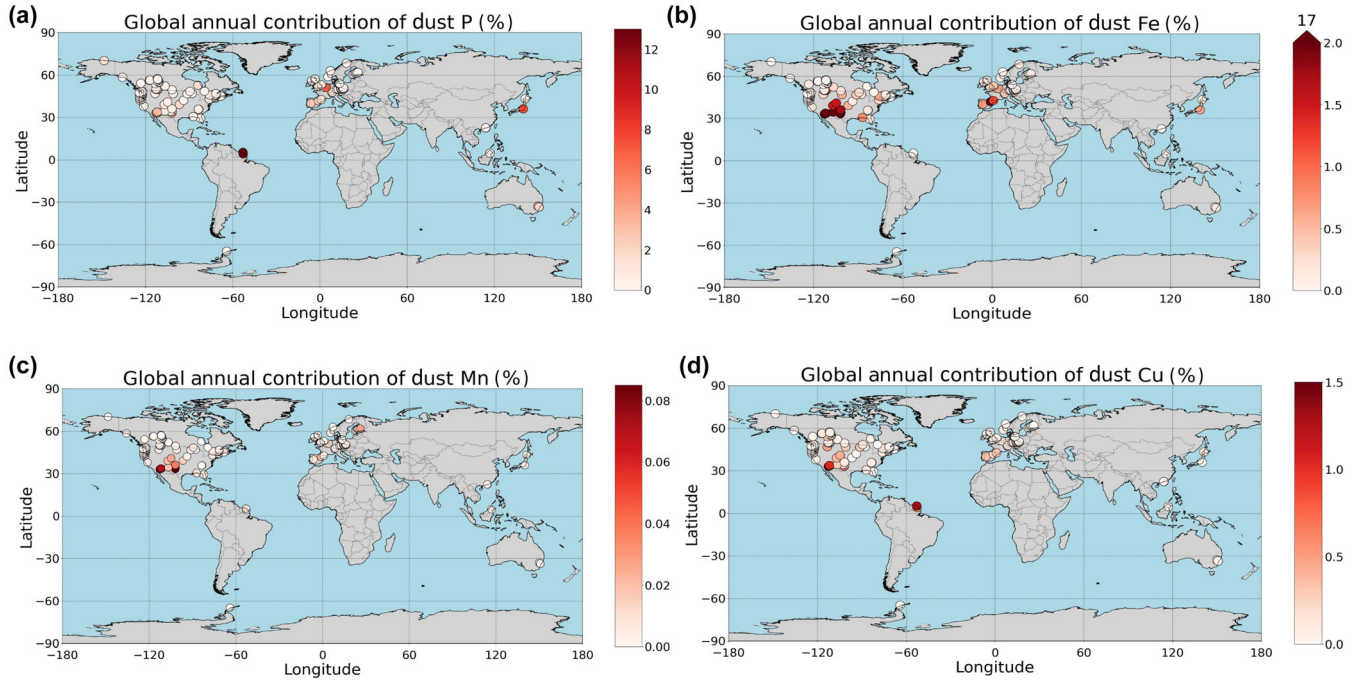

Fig. 6 Annual contribution of dust-derived nutrients relative to soil nutrient fluxes. Maps showing the modeled annual ratio (%) of bioavailable nutrients supplied by atmospheric dust deposition compared to nutrient fluxes measured with PRS™ membranes (Ochoa-Hueso *et al.*, 2023). Each circle marks a location where PRS data were available, and its color indicates the relative contribution of dust. Values represent the fraction of dust-derived bioavailable nutrient supply divided by the corresponding soil nutrient flux. (a) Dust Fe contribution. (b) Dust P contribution. (c) Dust Mn contribution. (d) Dust Cu contribution.

Mediterranean and semiarid regions, occurring on up to 50–70% of nights during the dry season, with typical water inputs ranging from 0.05 to 0.5 mm per event (Pina *et al.*, 2016). These processes were not included in the present study, which was designed to apply large, compositionally consistent quantities of dust with minimal atmospheric alteration. As such, the reported values likely underestimate the true bioavailability of dust-deposited nutrients.

The dust-derived nutrient deposition hotspots that appear in the Western United States and the Mediterranean result from high dust loads. By contrast, the emergence of a dust P deposition hotspot in the Eastern Amazon (Fig. 6d) reflects the extremely low bioavailable P fluxes in these highly weathered tropical soils (Cunha *et al.*, 2022; Reichert *et al.*, 2022). Under such conditions, even relatively small dust inputs become ecologically significant. The contribution of dust-derived P (*c.* 12% annually relative to soil-available fluxes) may help explain the large uncertainties in net primary productivity across parts of the eastern and central Amazon, where P limitation is known to be critical (e.g. Turner *et al.*, 2018; Cunha *et al.*, 2022; Nakhavali *et al.*, 2022; Goll *et al.*, 2023).

The contrasting responses between foliar and root–dust application indicate that nutrient uptake occurred primarily through direct foliar absorption. Limited root uptake can be attributed to the small dust-to-soil mass ratio, the low solubility of dust-borne nutrients under alkaline soil conditions, restricted root–dust contact, and potential competition with microorganisms or neighboring plants (Vitousek *et al.*, 2010; Marschner *et al.*, 2011; Arsic *et al.*, 2025). The pronounced increase in shoot micronutrient concentrations following foliar application, together with minimal changes in root nutrient levels and weak responses to root-applied dust, supports this interpretation and is consistent with previous glasshouse and controlled-environment studies demonstrating a dominant foliar uptake pathway for dust-derived nutrients (Gross *et al.*, 2021; Starr *et al.*, 2023; Lokshin *et al.*, 2024b, 2025).

To understand how dust-derived nutrients access internal leaf compartments, we next consider the physical and chemical pathways available for foliar uptake. Dissolution at the leaf surface followed by diffusion across the cuticle represents an important pathway for foliar nutrient uptake, as the cuticle, although largely hydrophobic, contains dynamic aqueous domains that permit the transport of dissolved solutes, particularly under humid conditions (Eichert & Fernández, 2023). Stomata may additionally provide access points for hydrophilic solutes or very fine particles; however, their effective contribution depends on particle size, pore geometry, and stomatal opening. Atmospheric mineral dust in Israel and the Eastern Mediterranean is dominated during dust events by particles within the PM size fraction, with substantial contributions from locally deposited coarse material (Ganor *et al.*, 2009), while the dust applied here (< 63 µm) represents a broad range of wind-transportable particles. Mediterranean shrub species typically exhibit predominantly abaxial stomatal distributions, as reported for *Salvia* and other Mediterranean taxa

© 2026 The Author(s).
New Phytologist © 2026 New Phytologist Foundation.

14698137, 0, Downloaded from https://nph.onlinelibrary.wiley.com/doi/10.1111/nph.71112 by CochraneAustria, Wiley Online Library on [08/04/2026]. See the Terms and Conditions (https://onlinelibrary.wiley.com/terms-and-conditions) on Wiley Online Library for rules of use; OA articles are governed by the applicable Creative Commons License

(Galmés *et al.*, 2006; Bercu *et al.*, 2012; Christodoulakis *et al.*, 2014), which may reduce the likelihood of direct particle entry from the usually dust-exposed adaxial surface. In addition to cuticular and stomatal pathways, leaf surface morphology likely plays a key role in foliar uptake: trichomes can enhance dust retention and prolong particle–leaf contact time, while structural discontinuities such as cracks at the trichome base may serve as localized entry points facilitating solute access to internal tissues, as previously suggested by Gross *et al.* (2021). Together, these pathways indicate that foliar nutrient acquisition from dust is governed by a combination of surface-mediated chemical processes and structural access points, whose relative contributions remain unresolved and warrant targeted mechanistic investigation.

Beyond entry into the leaf, the nutritional relevance of dust-derived elements depends on their subsequent fate within plant tissues. Our field experiment quantifies the fraction of dust-derived elements that becomes plant-associated relative to the total elemental content of the deposited dust, thereby demonstrating that atmospheric dust can provide a substantial and nutritionally meaningful contribution to plant nutrient supply. Although this approach does not resolve the detailed intracellular fate of individual elements, it clearly shows that a measurable proportion of dust-derived nutrients is mobilized from particles and retained by plant tissues.

The subsequent partitioning of these nutrients between extracellular compartments and metabolically active pools cannot be resolved here and represents an important direction for future research. Importantly, for metal micronutrients such as Fe, Mn, and Cu, nutritional effectiveness depends not only on uptake from dust but also on chemical speciation, as oxidized phases such as Fe^{3+} oxides may require further mobilization or complexation before metabolic utilization. Notably, the element-specific responses observed in this study, where certain nutrients increased more strongly than others rather than all elements increasing uniformly (Fig. S4), indicate that foliar acquisition from dust is not indiscriminate, but instead reflects selective and regulated processes at the leaf level.

Phosphorus deposition

Phosphorus deposition is hypothesized to play a critical role in stimulating ecosystem productivity, depending on location and plant traits (Yang *et al.*, 2025). Although we did not detect changes in leaf P concentrations following dust application, this is consistent with the high mobility of foliar-absorbed P, which is rapidly redistributed within plant tissues and does not accumulate at the site of uptake (Arsic *et al.*, 2025), unlike micronutrients that are typically immobile in shoots (Page & Feller, 2015). To place these uptake patterns in a mechanistic chemical context, we examined leaf surface chemistry. Consistent with previous findings that plants actively modulate leaf surface chemistry via organic acid exudation (Yoshida *et al.*, 1997; Gross *et al.*, 2021; Tang *et al.*, 2021; Golan *et al.*, 2025; Lokshin *et al.*, 2025), we detected organic acids on leaf surfaces across all species (Table S3). These compounds, including malic and citric acids, are known to promote the dissolution of micronutrients such as Fe, Mn, and P (Jauregui & Reisenauer, 1982; Hinsinger, 2001). The combination of moderately acidic leaf surfaces and the secretion of nutrient-solubilizing organic acids represents a widespread trait among many diverse plant species across ecosystems (Yoshida *et al.*, 1997; Gilbert & Renner, 2021; Tang *et al.*, 2021).

In earlier studies, foliar dust application enhanced total plant P uptake primarily through increased biomass production (Gross *et al.*, 2021; Starr *et al.*, 2023; Lokshin *et al.*, 2025). In the current study, however, elevated micronutrient concentrations and likely increased P uptake did not lead to measurable changes in biomass, root-to-shoot allocation, or leaf production (Figs S3, S4). Because plants in the field started from different initial sizes and grew under heterogeneous conditions, variation among individuals likely masked potential growth responses that were detectable under controlled laboratory experiments. Thus, while nutrient uptake clearly occurred, it did not translate into consistent biomass changes within the timeframe of this study. Detectable responses in plant physiology or growth to dust inputs may emerge later in the season or become more evident after multiple years of repeated deposition.

Dust deposition can also have a detrimental impact on plant physiology and growth through photosynthetic inhibition, caused by surface shading or partial stomatal occlusion, which may offset some of the observed nutritional benefits. Previous studies have reported minor reductions in carbon assimilation under heavy dust deposition (Moradi *et al.*, 2017; Starr *et al.*, 2023; Lokshin *et al.*, 2024a). While no signs of chlorosis or visible physiological stress were observed in the foliar-dusted plants in this study, indicating that dust application did not elicit strong negative effects on photosynthetic function, our study focused primarily on nutrient uptake. Future work should include targeted physiological measurements such as photosynthesis, stomatal conductance, and Chl fluorescence to directly quantify and mechanistically resolve potential trade-offs between foliar nutrient acquisition and photosynthetic performance.

Dust nutrient contribution per dust event basis

To further contextualize dust nutrient fluxes and given the episodic nature of dust events that occur in sporadic, high-intensity pulses, we also calculated the contribution of deposited nutrients on a per-event basis, defined here as a single dust deposition day ('dust day') based on regional dust climatology and event frequency (Ganor *et al.*, 2010). This allows estimation of nutrient inputs during discrete, high-deposition periods, rather than annual averages alone, and comparison to soil nutrient fluxes, which are more continuous and governed by slower biogeochemical processes. Our analysis focused on the Mediterranean region, which encompasses our study site and emerged as a hotspot for dust nutrient deposition (Fig. 5). We found that dust deposition can contribute up to 1000% of the daily bioavailable fluxes of Fe and P relative to soil fluxes, and up to 50 and 5% for Cu and Mn, respectively. These contributions exhibit a pronounced

© 2026 The Author(s).
New Phytologist © 2026 New Phytologist Foundation.

14698137, 0, Downloaded from https://nph.onlinelibrary.wiley.com/doi/10.1111/nph.71112 by CochraneAustria, Wiley Online Library on [08/04/2026]. See the Terms and Conditions (https://onlinelibrary.wiley.com/terms-and-conditions) on Wiley Online Library for rules of use; OA articles are governed by the applicable Creative Commons License

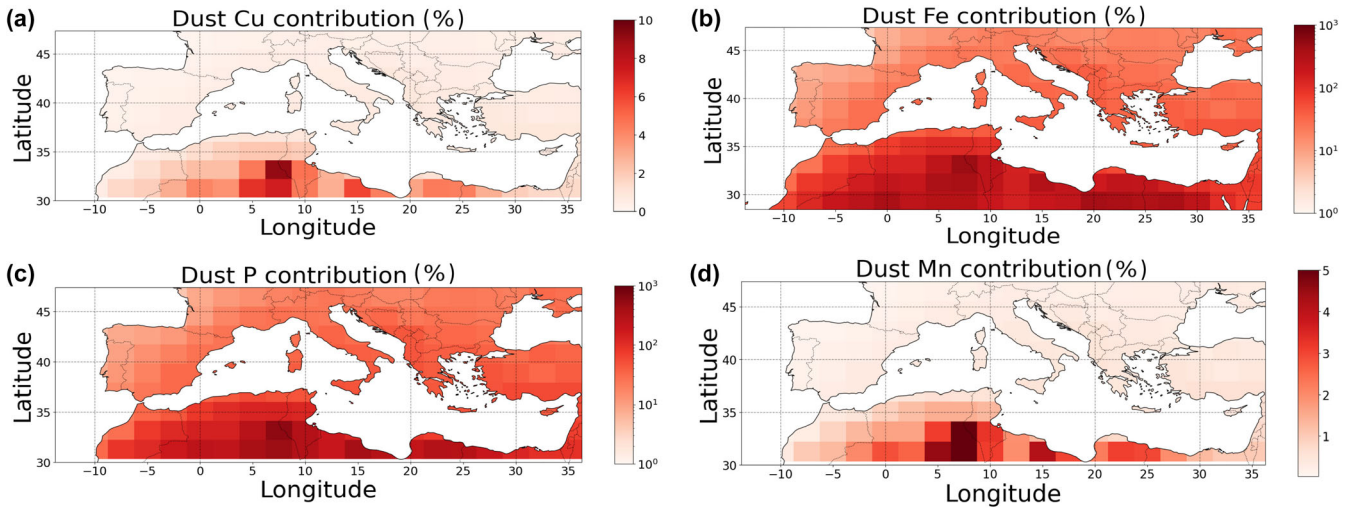

Fig. 7 Dust contribution to total bioavailable nutrient input on dust-event days across the Mediterranean. Maps show, for each nutrient, the dust-borne contribution expressed as the percentage of that day's total bioavailable nutrient flux on dust-event days. (a) Dust Fe contribution. (b) Dust P contribution. (c) Dust Mn contribution. (d) Dust Cu contribution. Warmer (reddish) colors indicate areas where episodic dust events account for a larger percentage contribution of dust relative to the combined dust and soil supply for each nutrient.

south-to-north impact gradient, reflecting proximity to major dust sources in the Sahara and Arabian deserts (Fig. 7a–d). While these event-scale fluxes clearly demonstrate the potential for dust deposition to dominate plant nutrient supply during dust days, the subsequent fate and physiological availability of dust-derived nutrients following foliar entry, including their retention in extracellular compartments and transport into metabolically active pools, remain important topics for future investigation.

Overall, our spatial analysis shows that the relative contribution of dust to plant nutrition varies regionally, following gradients in dust deposition and soil nutrient availability. In regions where dust deposition is high or soil nutrient bioavailability is particularly low, dust-borne nutrient fluxes during dust events may exceed those from the soil by orders of magnitude.

Given the projected changes in dust-emitting events driven by climate change, land degradation, and desert expansion (Kok *et al.*, 2023), dust nutrient deposition is likely to shape plant nutrition, terrestrial nutrient cycles, and ecosystem structure. However, important data gaps currently limit the accurate parameterization of atmospheric nutrient deposition in models. These include limited empirical measurements of leaf surface chemical composition and morphology across biomes, poor constraints on dust residence time on foliage under field conditions, and a lack of comparative data on plant functional traits that influence foliar nutrient uptake, such as trichome density, cuticle properties, and surface acidity. Canopy structures may further amplify dust deposition on foliage, as shown for fire-derived ash, where interception strongly increases with canopy complexity (Bauters *et al.*, 2021). Such amplification is likely to be particularly important in tropical forests (Hinko-Najera Umana & Wanek, 2010), where high leaf area and architectural complexity enhance particle trapping and where P limitation makes atmospheric nutrient inputs disproportionately valuable (Goll *et al.*, 2023). Addressing these gaps will require coordinated field campaigns across diverse ecosystems, targeted experiments manipulating dust characteristics and canopy traits, and standardized protocols to measure dust retention and uptake efficiency. Despite these limitations, our findings provide a mechanistic foundation for integrating dust-derived nutrient inputs into models of nutrient acquisition, species interactions, and ecosystem productivity (Jiang *et al.*, 2019). For example, state-of-the-art C–N–P models (e.g. JULES-CNP and CLM5-CNP) impose P or micronutrient limitation by routing all atmospheric inputs to the soil, where most nutrients are rapidly immobilized, leading to strong CO_2-fertilization damping (Fleischer *et al.*, 2019), especially in P-poor ecosystems such as the Amazon. Our results show that plants can bypass the soil bottleneck by directly absorbing dust-borne P (and co-deposited micronutrients) through their leaves, a pathway ignored in current modeling frameworks. To capture this overlooked feedback, models should treat dust deposition as a canopy resource as well as a soil input, allowing a fraction of deposited nutrients to enter the plants based on dust chemistry, leaf surface chemical and morphological traits, and residence time. This could ease nutrient shortfalls under elevated CO_2, improve predictions of productivity, and bring terrestrial carbon–nutrient feedback closer to observed ecosystem behavior.

Acknowledgements

This research was supported by the Israel Science Foundation (ISF 267/24; A. Gross) and by the Israel Science Foundation (ISF 3171/24; TG). The Matta LTER station received support from the Ministry of Science, Technology and Space (grant no. 314442 to MS) and the Chief Scientist of the Jewish National Fund (grant no. 1823 to MS). We thank Mr. Idan Ben Altar for assistance with geospatial analysis and Mrs. Neta Sotto and Mrs.

© 2026 The Author(s).
New Phytologist © 2026 New Phytologist Foundation.

14698137, 0, Downloaded from https://nph.onlinelibrary.wiley.com/doi/10.1111/nph.71112 by CochraneAustria, Wiley Online Library on [08/04/2026]. See the Terms and Conditions (https://onlinelibrary.wiley.com/terms-and-conditions) on Wiley Online Library for rules of use; OA articles are governed by the applicable Creative Commons License

Noa Naiman for their help with the field experiment. TG acknowledges support from the Council for Higher Education of Israel through the climate science call, under the project "Integrating Climate Dynamics, Clouds, and Extreme Events through Teleconnections in Climate Networks. MAN acknowledges Funding from the European Commission under the scope of the ForestNavigator project (grant agreement No 101056875).

Competing interests

None declared.

Author contributions

AL, AG and DP conceptualized the study and designed the field experiment. AL, AG and DP conducted the fieldwork, with ecological input, species selection, and biomass and growth sampling provided by MS, who leads the Matta LTER site. Chemical analyses were performed by AL, AG, DP and MS The geospatial model was developed primarily by TG, with contributions from AL and AG. AG acquired funding and, together with DP, led project administration and supervised the research. AL, AG and DP wrote the original draft, with MAN contributing to writing and text development. All authors contributed to reviewing and editing the manuscript.

ORCID

Tom Goren https://orcid.org/0000-0001-5618-9402
Avner Gross https://orcid.org/0000-0001-8425-8508
Anton Lokshin https://orcid.org/0009-0007-3946-6341
Mahdi (André) Nakhavali https://orcid.org/0000-0003-2675-6730
Daniel Palchan https://orcid.org/0000-0002-7320-4085
Marcelo Sternberg https://orcid.org/0000-0001-8710-4141

Data availability

All data supporting the findings of this study are available within the paper and its Supplementary Information files. The data that support the findings of this study are available in 10.5281/zenodo.19064951.

References

Adar S, Sternberg M. 2026. Evaluating microclimatic alterations under rainout shelters: Intended and unintended effects of drought manipulations. *Ecological Applications* **36**: e70172.

Adebiyi AA, Kok JF. 2020. Climate models miss most of the coarse dust in the atmosphere. *Science Advances* **6**: 1–9.

Alon M, Sternberg M. 2019. Effects of extreme drought on primary production, species composition and species diversity of a Mediterranean annual plant community. *Journal of Vegetation Science* **30**: 1045–1061.

Arsic M, Howell NR, Cresswell T, Brunetti G, Husted S, Schjoerring JK, Persson DP, Lombi E, Doolette CL. 2025. Effects of phosphorus deficiency on leaf surface morphology: absorption and translocation of foliar-applied phosphorus in four barley cultivars. *Physiologia Plantarum* **177**: e70263.

Arvin LJ, Riebe CS, Aciego SM, Blakowski MA. 2017. Global patterns of dust and bedrock nutrient supply to montane ecosystems. *Science Advances* **3**: 1–11.

Baker AR, Kanakidou M, Nenes A, Myriokefalitakis S, Croot PL, Duce RA, Gao Y, Guieu C, Ito A, Jickells TD *et al.* 2021. Changing atmospheric acidity as a modulator of nutrient deposition and ocean biogeochemistry. *Science Advances* **7**: 1–9.

Barr SL, Wyld B, McQuaid JB, Neely RR, Murray BJ. 2023. Southern Alaska as a source of atmospheric mineral dust and ice-nucleating particles. *Science Advances* **9**: eadg3708.

Barrat JA, Zanda B, Moynier F, Bollinger C, Liorzou C, Bayon G. 2012. Geochemistry of CI chondrites: major and trace elements, and Cu and Zn isotopes. *Geochimica et Cosmochimica Acta* **83**: 79–92.

Bauters M, Drake TW, Wagner S, Baumgartner S, Makelele IA, Bodé S, Verheyen K, Verbeeck H, Ewango C, Cizungu L *et al.* 2021. Fire-derived phosphorus fertilization of African tropical forests. *Nature Communications* **12**: 1–8.

Bercu R, Negrean G, Broască L. 2012. Leaf anatomical study of taxons *Salvia nemorosa* subsp. *tesquicola*, *Salvia nutans*, and *Salvia* × sobrogensis from Dobrudja. *Botanica Serbica* **36**: 103–109.

Blanckaert ACA, Omanović D, Fine M, Grover R, Ferrier-Pagès C. 2022. Desert dust deposition supplies essential bioelements to Red Sea corals. *Global Change Biology* **28**: 2341–2359.

Blanusa T, Fantozzi F, Monaci F, Bargagli R. 2015. Leaf trapping and retention of particles by holm oak and other common tree species in Mediterranean urban environments. *Urban Forestry & Urban Greening* **14**: 1095–1101.

Brahney J, Heindel RC, Gill TE, Carling G, González-Olalla JM, Hand J, Mallia DV, Munroe JS, Perry K, Putman AL *et al.* 2024. Dust in the Critical Zone: North American case studies. *Earth-Science Reviews* **258**: 104942.

Bristow CS, Hudson-Edwards KA, Chappell A. 2010. Fertilizing the Amazon and equatorial Atlantic with West African dust. *Geophysical Research Letters* **37**: L14807.

Bukovac MJ, Wittwer SH. 1957. Absorption and mobility of foliar applied nutrients. *Plant Physiology* **32**: 428–435.

Censi P, Cibella F, Falcone EE, Cuttitta G, Saiano F, Inguaggiato C, Latteo V. 2017. Rare earths and trace elements contents in leaves: a new indicator of the composition of atmospheric dust. *Chemosphere* **169**: 342–350.

Chadwick OA, Derry LA, Vitousek PM, Huebert BJ, Hedin LO. 1999. Changing sources of nutrients during four million years of ecosystem development. *Nature* **397**: 491–497.

Christodoulakis NS, Georgoudi M, Fasseas C. 2014. Leaf structure of *Cistus creticus* L. (rock rose), a medicinal plant widely used in folk remedies since ancient times. *Journal of Herbs Spices & Medicinal Plants* **20**: 103–114.

Cunha HFV, Andersen KM, Lugli LF, Santana FD, Aleixo IF, Moraes AM, Garcia S, Di Ponzio R, Mendoza EO, Brum B *et al.* 2022. Direct evidence for phosphorus limitation on Amazon forest productivity. *Nature* **608**: 558–562.

Dam TTN, Angert A, Krom MD, Bigio L, Hu Y, Beyer KA, Mayol-Bracero OL, Santos-Figueroa G, Pio C, Zhu M. 2021. X-ray spectroscopic quantification of phosphorus transformation in Saharan dust during *trans*-Atlantic dust transport. *Environmental Science and Technology* **55**: 12694–12703.

Dayan U, Ziv B, Shoob T, Enzel Y. 2008. Suspended dust over southeastern Mediterranean and its relation to atmospheric circulations. *International Journal of Climatology* **28**: 915–924.

Eichert T, Fernández V. 2023. Uptake and release of elements by leaves and other aerial plant parts. In: Marschner P, ed. *Marschner's mineral nutrition of plants*. London, UK: Academic Press, 105–129.

Elderfield H, Whitfield M, Burton JD, Bacon MP, Liss PS. 1988. The oceanic chemistry of the rare-earth elements. *Philosophical Transactions of the Royal Society of London. Series B: Biological Sciences* **325**: 105–126.

Fernández V, Brown PH. 2013. From plant surface to plant metabolism: the uncertain fate of foliar-applied nutrients. *Frontiers in Plant Science* **4**: 1–5.

Fernandez V, Eichert T. 2009. Uptake of hydrophilic solutes through plant leaves: current state of knowledge and perspectives of foliar fertilization. *Critical Reviews in Plant Sciences* **28**: 36–68.

Fleischer K, Rammig A, De Kauwe MG, Walker AP, Domingues TF, Fuchslueger L, Garcia S, Goll DS, Grandis A, Jiang M *et al.* 2019. Amazon

© 2026 The Author(s).
New Phytologist © 2026 New Phytologist Foundation.

14698137, 0, Downloaded from https://nph.onlinelibrary.wiley.com/doi/10.1111/nph.71112 by CochraneAustria, Wiley Online Library on [08/04/2026]. See the Terms and Conditions (https://onlinelibrary.wiley.com/terms-and-conditions) on Wiley Online Library for rules of use; OA articles are governed by the applicable Creative Commons License

forest response to CO_2 fertilization dependent on plant phosphorus acquisition. *Nature Geoscience* **12**: 736–741.

Galmés J, Flexas J, Savé R, Medrano H. 2006. Water relations and stomatal characteristics of Mediterranean plants with different growth forms and leaf habits: responses to water stress and recovery. *Plant and Soil* **290**: 139–155.

Ganor E, Foner HA. 2001. Mineral dust concentrations, deposition fluxes and deposition velocities in dust episodes over Israel. *Journal of Geophysical Research: Atmospheres* **106**: 18431–18437.

Ganor E, Osetinsky I, Stupp A, Alpert P. 2010. Increasing trend of African dust, over 49 years, in the eastern Mediterranean. *Journal of Geophysical Research: Atmospheres* **115**: 7201.

Ganor E, Stupp A, Alpert P. 2009. A method to determine the effect of mineral dust aerosols on air quality. *Atmospheric Environment* **43**: 5463–5468.

Gilbert KJ, Renner T. 2021. Acid or base? How do plants regulate the ecology of their phylloplane? *AoB Plants* **13**: plab032.

Golan E, Gross A, Agam N, Yasuor H, Shtein I, Erel R. 2025. Leaf chemical and structural properties govern foliar uptake of phosphorus from dust in chickpea. *Environmental and Experimental Botany* **236**: 106168.

Goll DS, Bauters M, Zhang H, Ciais P, Balkanski Y, Wang R, Verbeeck H. 2023. Atmospheric phosphorus deposition amplifies carbon sinks in simulations of a tropical forest in Central Africa. *New Phytologist* **237**: 2054–2068.

Gross A, Goren T, Pio C, Cardoso J, Tirosh O, Todd MC, Rosenfeld D, Weiner T, Custódio D, Angert A. 2015. Variability in sources and concentrations of saharan dust phosphorus over the Atlantic Ocean. *Environmental Science and Technology Letters* **2**: 31–37.

Gross A, Tiwari S, Shtein I, Erel R. 2021. Direct foliar uptake of phosphorus from desert dust. *New Phytologist* **230**: 2213–2225.

Gross A, Turner BL, Goren T, Berry A, Angert A. 2016. Tracing the sources of atmospheric phosphorus deposition to a tropical rain forest in Panama using stable oxygen isotopes. *Environmental Science and Technology* **50**: 1147–1156.

Guieu C, Dulac F, Ridame C, Pondaven P. 2014. Introduction to project DUNE, a DUst experiment in a low nutrient, low chlorophyll ecosystem. *Biogeosciences* **11**: 425–442.

Guinoiseau D, Singh SP, Galer SJG, Abouchami W, Bhattacharyya R, Kandler K, Bristow C, Andreae MO. 2022. Characterization of Saharan and Sahelian dust sources based on geochemical and radiogenic isotope signatures. *Quaternary Science Reviews* **293**: 107729.

Hinko-Najera Umana N, Wanek W. 2010. Large canopy exchange fluxes of inorganic and organic nitrogen and preferential retention of nitrogen by epiphytes in a tropical lowland rainforest. *Ecosystems* **13**: 367–381.

Hinsinger P. 2001. Bioavailability of soil inorganic P in the rhizosphere as affected by root-induced chemical changes: a review. *Plant and Soil* **237**: 173–195.

Holzapfel C, Tielbörger K, Parag HA, Kigel J, Sternberg M. 2006. Annual plant–shrub interactions along an aridity gradient. *Basic and Applied Ecology* **7**: 268–279.

Jauregui MA, Reisenauer HM. 1982. Dissolution of oxides of manganese and iron by root exudate components. *Soil Science Society of America Journal* **46**: 314–317.

Jiang M, Caldararu S, Zaehle S, Ellsworth DS, Medlyn BE. 2019. Towards a more physiological representation of vegetation phosphorus processes in land surface models. *New Phytologist* **222**: 1223–1229.

Jickells TD, An ZS, Andersen KK, Baker AR, Bergametti G, Brooks N, Cao JJ, Boyd PW, Duce RA, Hunter KA *et al.* 2005. Global iron connections between desert dust, ocean biogeochemistry, and climate. *Science* **308**: 67–71.

Jones DL. 1998. Organic acids in the rhizosphere–a critical review. *Plant and Soil* **205**: 25–44.

Kok JF, Adebiyi AA, Albani S, Balkanski Y, Checa-Garcia R, Chin M, Colarco PR, Hamilton DS, Huang Y, Ito A *et al.* 2021. Contribution of the world's main dust source regions to the global cycle of desert dust. *Atmospheric Chemistry and Physics* **21**: 8169–8193.

Kok JF, Ridley DA, Zhou Q, Miller RL, Zhao C, Heald CL, Ward DS, Albani S, Haustein K. 2017. Smaller desert dust cooling effect estimated from analysis of dust size and abundance. *Nature Geoscience* **10**: 274–278.

Kok JF, Storelvmo T, Karydis VA, Adebiyi AA, Mahowald NM, Evan AT, He C, Leung DM. 2023. Mineral dust aerosol impacts on global climate and climate change. *Nature Reviews Earth and Environment* **4**: 71–86.

Laveuf C, Cornu S. 2009. A review on the potentiality of rare earth elements to trace pedogenetic processes. *Geoderma* **154**: 1–12.

Li W, Xu L, Liu X, Zhang J, Lin Y, Yao X, Gao H, Zhang D, Chen J, Wang W *et al.* 2017. Air pollution–aerosol interactions produce more bioavailable iron for ocean ecosystems. *Science Advances* **3**: 1–6.

Liang T, Ding S, Song W, Chong Z, Zhang HC, Li H. 2008. A review of fractionations of rare earth elements in plants. *Journal of Rare Earths* **26**: 7–15.

Lindsay WL, Norvell WA. 1978. Development of a DTPA soil test for zinc, iron, manganese, and copper. *Soil Science Society of America Journal* **42**: 421–428.

Lokshin A, Gross A, Dor YB, Palchan D. 2024a. Rare earth elements as a tool to study the foliar nutrient uptake phenomenon under ambient and elevated atmospheric CO_2 concentration. *Science of the Total Environment* **948**: 174695.

Lokshin A, Palchan D, Golan E, Erel R, Andronico D, Gross A. 2025. Foliar nutrient uptake from dust sustains plant nutrition. *Biogeosciences* **22**: 2653–2666.

Lokshin A, Palchan D, Gross A. 2024b. Direct foliar phosphorus uptake from wildfire ash. *Biogeosciences* **21**: 2355–2365.

Lu L, Li L, Rathod S, Hess P, Martínez C, Fernandez N, Goodale C, Thies J, Wong MY, Alaimo MG *et al.* 2024. Characterizing the atmospheric Mn cycle and its impact on terrestrial biogeochemistry. *Global Biogeochemical Cycles* **38**: e2023GB007967.

Mahowald NM, Hamilton DS, Mackey KRM, Moore JK, Baker AR, Scanza RA, Zhang Y. 2018. Aerosol trace metal leaching and impacts on marine microorganisms. *Nature Communications* **9**: 2614.

Marschner P, Crowley D, Rengel Z. 2011. Rhizosphere interactions between microorganisms and plants govern iron and phosphorus acquisition along the root axis – model and research methods. *Soil Biology and Biochemistry* **43**: 883–894.

Matos IS, Binks O, Eller CB, Zorger BB, Meir P, Dawson TE, Rosado BHP. 2022. Revisiting plant hydrological niches: the importance of atmospheric resources for ground-rooted plants. *Journal of Ecology* **110**: 1746–1756.

Matzenbacher BA, Brummer GJA, Prins MA, Stuut JBW. 2024. High-resolution sampling in the eastern tropical North Atlantic reveals episodic Saharan dust deposition: implications for the marine carbon sink. *Frontiers in Marine Science* **11**: 1367786.

Mo L, Ma Z, Xu Y, Sun F, Lun X, Liu X, Chen J, Yu X. 2015. Assessing the capacity of plant species to accumulate particulate matter in Beijing, China. *PLoS ONE* **10**: e0140664.

Molina Catricheo CA, Lambert F, Salomon J, van't Wout E. 2024. Modeling global surface dust deposition using physics-informed neural networks. *Communications Earth & Environment* **5**: 778.

Moradi A, Taheri Abkenar K, Afshar Mohammadian M, Shabanian N. 2017. Effects of dust on forest tree health in Zagros oak forests. *Environmental Monitoring and Assessment* **189**: 549.

Moreno T, Querol X, Castillo S, Alastuey A, Cuevas E, Herrmann L, Mounkaila M, Elvira J, Gibbons W. 2006. Geochemical variations in aeolian mineral particles from the Sahara-Sahel Dust Corridor. *Chemosphere* **65**: 261–270.

Moreno-Jiménez E, Plaza C, Saiz H, Manzano R, Flagmeier M, Maestre FT. 2019. Aridity and reduced soil micronutrient availability in global drylands. *Nature Sustainability* **2**: 371–377.

Nakhavali MA, Mercado LM, Hartley IP, Sitch S, Cunha FV, di Ponzio R, Lugli LF, Quesada CA, Andersen KM, Chadburn SE *et al.* 2022. Representation of the phosphorus cycle in the Joint UK land environment simulator (vn5.5_JULES-CNP). *Geoscientific Model Development* **15**: 5241–5269.

Navarro-Pedreño J, Almendro-Candel MB, Lucas IG, Vidal MMJ, Borras JB, Zorpas AA. 2018. Trace metal content and availability of essential metals in agricultural soils of alicante (Spain). *Sustainability* **10**: 4534.

Nezat CA, Blum JD, Yanai RD, Hamburg SP. 2007. A sequential extraction to determine the distribution of apatite in granitoid soil mineral pools with application to weathering at the Hubbard Brook Experimental Forest, NH, USA. *Applied Geochemistry* **22**: 2406–2421.

Ochoa-Hueso R, Delgado-Baquerizo M, Risch AC, Ashton L, Augustine D, Bélanger N, Bridgham S, Britton AJ, Bruckman VJ, Camarero JJ *et al.* 2023.

© 2026 The Author(s).
New Phytologist © 2026 New Phytologist Foundation.

14698137, 0, Downloaded from https://nph.onlinelibrary.wiley.com/doi/10.1111/nph.71112 by CochraneAustria, Wiley Online Library on [08/04/2026]. See the Terms and Conditions (https://onlinelibrary.wiley.com/terms-and-conditions) on Wiley Online Library for rules of use; OA articles are governed by the applicable Creative Commons License

Bioavailability of macro and micronutrients across global topsoils: main drivers and global change impacts. *Global Biogeochemical Cycles* **37**: e2022GB007680.

Page V, Feller U. 2015. Heavy metals in crop plants: transport and redistribution processes on the whole plant level. *Agronomy* **5**: 447–463.

Palchan D, Erel Y, Stein M. 2018. Geochemical characterization of contemporary fine detritus in the Dead Sea watershed. *Chemical Geology* **494**: 30–42.

Paytan A, Mackey KRM, Chen Y, Lima ID, Doney SC, Mahowald N, Labiosa R, Post AF. 2009. Toxicity of atmospheric aerosols on marine phytoplankton. *Proceedings of the National Academy of Sciences, USA* **106**: 4601–4605.

Peel MC, Finlayson BL, McMahon TA. 2007. Updated world map of the Köppen-Geiger climate classification. *Hydrology and Earth System Sciences* **11**: 1633–1644.

Pett-Ridge JC. 2009. Contributions of dust to phosphorus cycling in tropical forests of the Luquillo Mountains, Puerto Rico. *Biogeochemistry* **94**: 63–80.

Pina ALCB, Zandavalli BRB, Oliveira RS, Martins FR, Soares AA. 2016. Dew absorption by the leaf trichomes of *Combretum leprosum* in the Brazilian semiarid region. *Functional Plant Biology* **43**: 199–208.

Rashid A, Ryan J. 2004. Micronutrient constraints to crop production in soils with mediterranean-type characteristics: a review. *Journal of Plant Nutrition* **27**: 959–975.

Reichert T, Rammig A, Fuchslueger L, Lugli LF, Quesada CA, Fleischer K. 2022. Plant phosphorus-use and -acquisition strategies in Amazonia. *New Phytologist* **234**: 1126–1143.

Rubin M, Berman-Frank I, Shaked Y. 2011. Dust- and mineral-iron utilization by the marine dinitrogen-fixer Trichodesmium. *Nature Geoscience* **4**: 529–534.

Smith FA. 2007. Plant roots. Growth, activity and interaction with soils. *Annals of Botany* **100**: 151–152.

Starr M, Klein T, Gross A. 2023. Direct foliar acquisition of desert dust phosphorus fertilizes forest trees despite reducing photosynthesis. *Tree Physiology* **43**: 794–804.

Stockdale A, Krom MD, Mortimer RJG, Benning LG, Carslaw KS, Herbert RJ, Shi Z, Myriokefalitakis S, Kanakidou M, Nenes A. 2016. Understanding the nature of atmospheric acid processing of mineral dusts in supplying bioavailable phosphorus to the oceans. *Proceedings of the National Academy of Sciences, USA* **113**: 14639–14644.

Tang S, Liu J, Lambers H, Zhang L, Liu Z, Lin Y, Kuang Y. 2021. Increase in leaf organic acids to enhance adaptability of dominant plant species in karst habitats. *Ecology and Evolution* **11**: 10277–10289.

Tielbörger K, Bilton MC, Metz J, Kigel J, Holzapfel C, Lebrija-Trejos E, Konsens I, Parag HA, Sternberg M. 2014. Middle-Eastern plant communities tolerate 9 years of drought in a multi-site climate manipulation experiment. *Nature Communications* **5**: 5102.

Tiwari S, Erel R, Gross A. 2022. Chemical processes in receiving soils accelerate solubilisation of phosphorus from desert dust and fire ash. *European Journal of Soil Science* **73**: e13270.

Turner BL, Brenes-Arguedas T, Condit R. 2018. Pervasive phosphorus limitation of tree species but not communities in tropical forests. *Nature* **555**: 367–370.

Uni D, Katra I. 2017. Airborne dust absorption by semi-arid forests reduces PM pollution in nearby urban environments. *Science of the Total Environment* **598**: 984–992.

Van Langenhove L, Verryckt LT, Bréchet L, Courtois EA, Stahl C, Hofhansl F, Bauters M, Sardans J, Boeckx P, Fransen E *et al.* 2020. Atmospheric deposition of elements and its relevance for nutrient budgets of tropical forests. *Biogeochemistry* **149**: 175–193.

Villanueva D, Stengel M, Hoose C, Bruno O, Jeggle K, Ansmann A, Lohmann U. 2025. Dust-driven droplet freezing explains cloud-top phase in the northern extratropics. *Science* **389**: 521–525.

Vitousek PM, Porder S, Houlton BZ, Chadwick OA. 2010. Terrestrial phosphorus limitation: mechanisms, implications, and nitrogen-phosphorus interactions. *Ecological Applications* **20**: 5–15.

Weis J, Chase Z, Schallenberg C, Strutton PG, Bowie AR, Fiddes SL. 2024. One-third of Southern Ocean productivity is supported by dust deposition. *Nature* **629**: 603–608.

Westberry TK, Behrenfeld MJ, Shi YR, Yu H, Remer LA, Bian H. 2023. Atmospheric nourishment of global ocean ecosystems. *Science* **380**: 515–519.

Yang N, Zohner CM, Crowther TW, Feng J, Wu J, Chen X, Han W, Stocker BD, Hui D, Augusto L *et al.* 2025. Leaf economic strategies drive global variation in phosphorus stimulation of terrestrial plant production. *Nature Communications* **16**: 5562.

Yoshida M, Cowgill SE, Wightman JA. 1997. Roles of oxalic and malic acids in chickpea trichome exudate in host-plant resistance to *Helicoverpa armigera*. *Journal of Chemical Ecology* **23**: 1195–1210.

Yusupov DV, Baranovskaya NV, Robertus YV, Radomskaya VI, Pavlova LM, Sudyko AF, Rikhvanov LP. 2020. Rare earth elements in poplar leaves as indicators of geological environment and technogenesis. *Environmental Science and Pollution Research* **27**: 27111–27123.

Zhang Y, Mahowald N, Scanza RA, Journet E, Desboeufs K, Albani S, Kok JF, Zhuang G, Chen Y, Cohen DD *et al.* 2015. Modeling the global emission, transport and deposition of trace elements associated with mineral dust. *Biogeosciences* **12**: 5771–5792.

Supporting Information

Additional Supporting Information may be found online in the Supporting Information section at the end of the article.

Fig. S1 Shoot nutrient concentrations of elements not consistently affected by dust treatments.

Fig. S2 Root nutrient concentrations following foliar and root dust application.

Fig. S3 Plant biomass responses to foliar dust application.

Fig. S4 Vegetative growth responses to foliar dust application.

Fig. S5 Soil nutrient concentrations beneath control and dust-treated plants.

Fig. S6 Contamination analysis of shoot nutrient concentrations.

Fig. S7 Global distribution of annual soil bioavailable nutrient fluxes.

Table S1 Soil physicochemical properties at the experimental site.

Table S2 Bioavailable nutrient concentrations in surface soils.

Table S3 Relative abundances of organic acids on leaf surfaces of three Mediterranean plant species.

Table S4 Dust characterization by X-ray fluorescence (XRF), X-ray diffraction (XRD), and inductively coupled plasma mass spectrometry.

Table S5 Field-based calculation of bioavailable fractions of each element and The percentage of nutrient foliar uptake, together with an associated uncertainty calculation for Fe, Mn, Cu, and P.

Table S6 Concentrations of rare earth elements (REEs) in plant tissues (shoots and roots).

© 2026 The Author(s).
New Phytologist © 2026 New Phytologist Foundation.

14698137, 0, Downloaded from https://nph.onlinelibrary.wiley.com/doi/10.1111/nph.71112 by CochraneAustria, Wiley Online Library on [08/04/2026]. See the Terms and Conditions (https://onlinelibrary.wiley.com/terms-and-conditions) on Wiley Online Library for rules of use; OA articles are governed by the applicable Creative Commons License

Please note: Wiley is not responsible for the content or functionality of any Supporting Information supplied by the authors. Any queries (other than missing material) should be directed to the *New Phytologist* Central Office.

Disclaimer: The New Phytologist Foundation remains neutral with regard to jurisdictional claims in maps and in any institutional affiliations.

14698137, 0, Downloaded from https://nph.onlinelibrary.wiley.com/doi/10.1111/nph.71112 by CochraneAustria, Wiley Online Library on [08/04/2026]. See the Terms and Conditions (https://onlinelibrary.wiley.com/terms-and-conditions) on Wiley Online Library for rules of use; OA articles are governed by the applicable Creative Commons License

© 2026 The Author(s).
New Phytologist © 2026 New Phytologist Foundation.